

LIGHT-CONE 2023

CBPF September 18-22, 2023

Vermelha Beach

Light-Cone 2023: Hadrons and Symmetries

Rio de Janeiro, September 18-22, 2023



CBPF

CENTRO BRASILEIRO DE PESQUISAS FÍSICAS

Beyond valence distributions in meson with Basis Light-front Quantization

Jiangshan Lan

With:

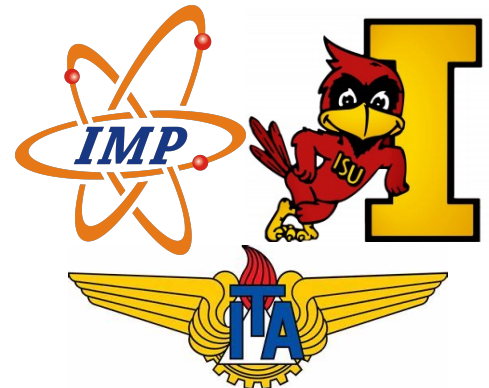
J. Wu, K. Fu, Z. Zhang, Z. Zhu, J. Chen, E. Ydrefors, C. Mondal, X. Zhao,
T. Frederico and J. P. Vary

Institute of Modern Physics, CAS, Lanzhou, China

Instituto Tecnológico de Aeronautica, Sao Jose dos Campos, Brazil

Iowa State University, Ames, US

Rio de Janeiro • September 19, 2023



06/04/2023 Excursion

Liujiaxia Reservoir
Elevation ~ 2050m



Outline

- Basis Light-front Quantization approach
- Application to Light Mesons
 - A review of BLFQ-NJL
 - Light mesons with one dynamical gluon
(LFWF, EMFF, PDA, PDF, GPD & TMD)
 - The pion $q\bar{q}g$ BLFQ .vs. BSE
- Application to Strangeonia and Strange mesons
- Conclusion & Outlook

Basis Light-front Quantization

[Vary et al, 2008]

- Nonperturbative eigenvalue problem

$$P^- |\beta\rangle = P_\beta^- |\beta\rangle$$

- P^- : light-front Hamiltonian
- $|\beta\rangle$: mass eigenstate
- P_β^- : eigenvalue for $|\beta\rangle$

- Evaluate observables for eigenstate

$$O \equiv \langle \beta | \hat{O} | \beta \rangle$$

- Fock sector expansion

- Eg. $|\text{meson}\rangle = a|q\bar{q}\rangle + b|q\bar{q}g\rangle + c|q\bar{q}q\bar{q}\rangle + d|q\bar{q}gg\rangle + \dots$



$$|\text{Baryon}\rangle = a|qqq\rangle + b|qqqg\rangle + c|qqq\bar{q}q\rangle + d|qqqgg\rangle + \dots$$

Siqi Xu, Wednesday at 9:30

- Discretized basis

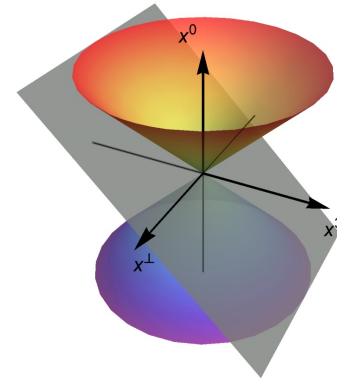
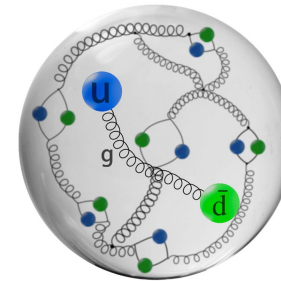
- Transverse: 2D harmonic oscillator basis: $\Phi_{n,m}^b(\vec{p}_\perp)$.
- Longitudinal: plane-wave basis, labeled by k .
- Basis truncation:

$$\sum_i (2n_i + |m_i| + 1) \leq N_{max},$$

$$\sum_i k_i = K.$$

N_{max}, K are basis truncation parameters.

Large N_{max} and K : High UV cutoff & low IR cutoff



Take a review

PDFs for Light Mesons

$$|\text{meson}\rangle = |q\bar{q}\rangle + \dots$$

$$H_{\text{eff}} = \frac{\vec{k}_{\perp}^2 + m_q^2}{x} + \frac{\vec{k}_{\perp}^2 + m_{\bar{q}}^2}{1-x} + \kappa^4 x(1-x) \vec{r}_{\perp}^2 - \frac{\kappa^4}{(m_q + m_{\bar{q}})^2} \partial_x (x(1-x) \partial_x) + H_{\text{eff}}^{\text{NJL}}$$

Diagonalizing H_{eff}



LF wave function

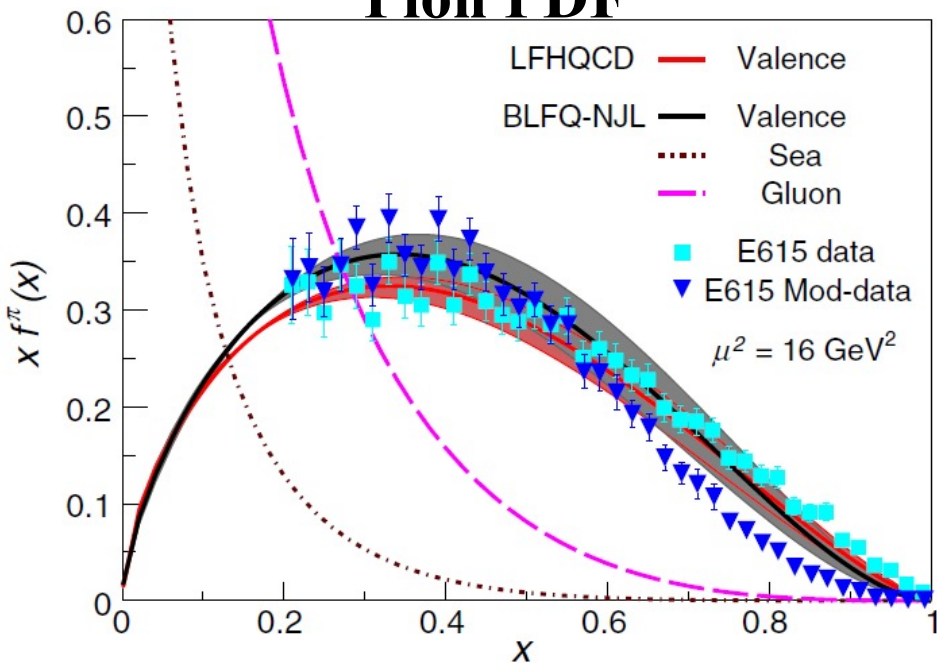


Initial PDFs

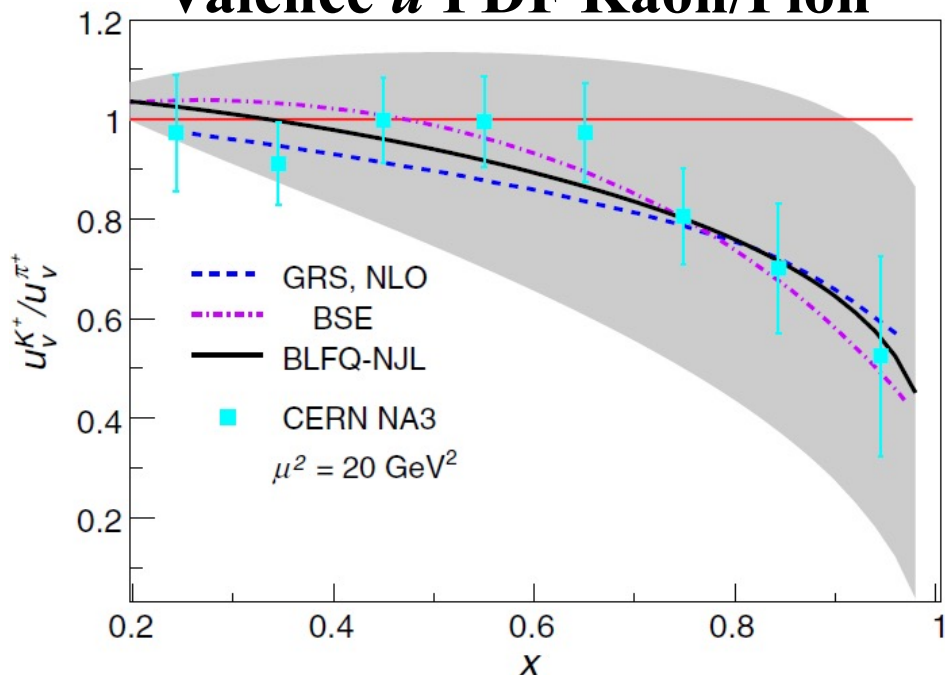


Scale evolution

Pion PDF

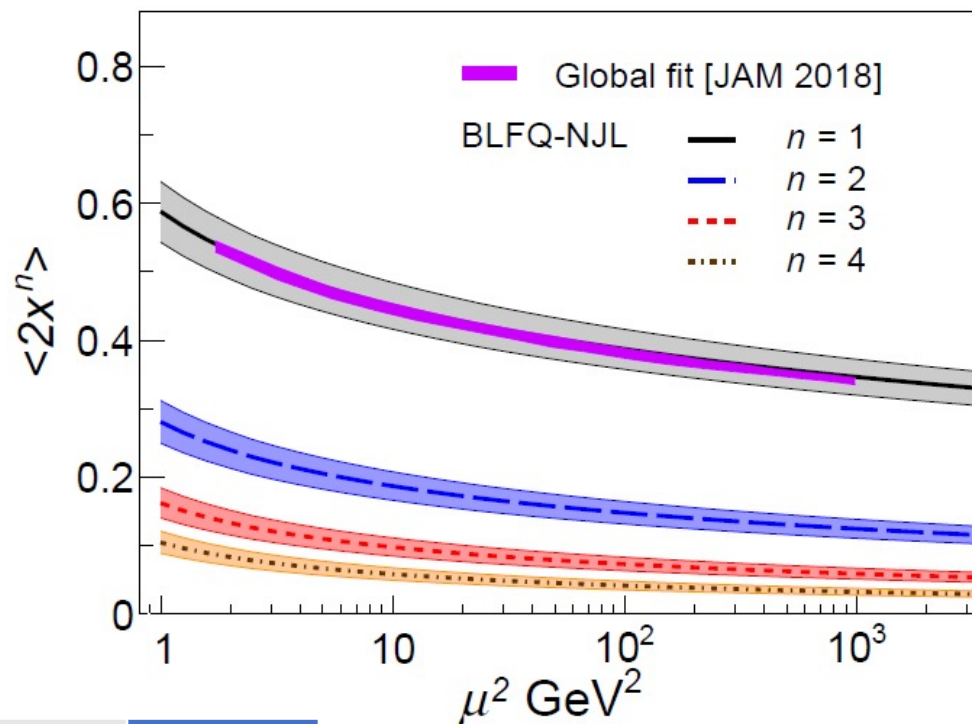
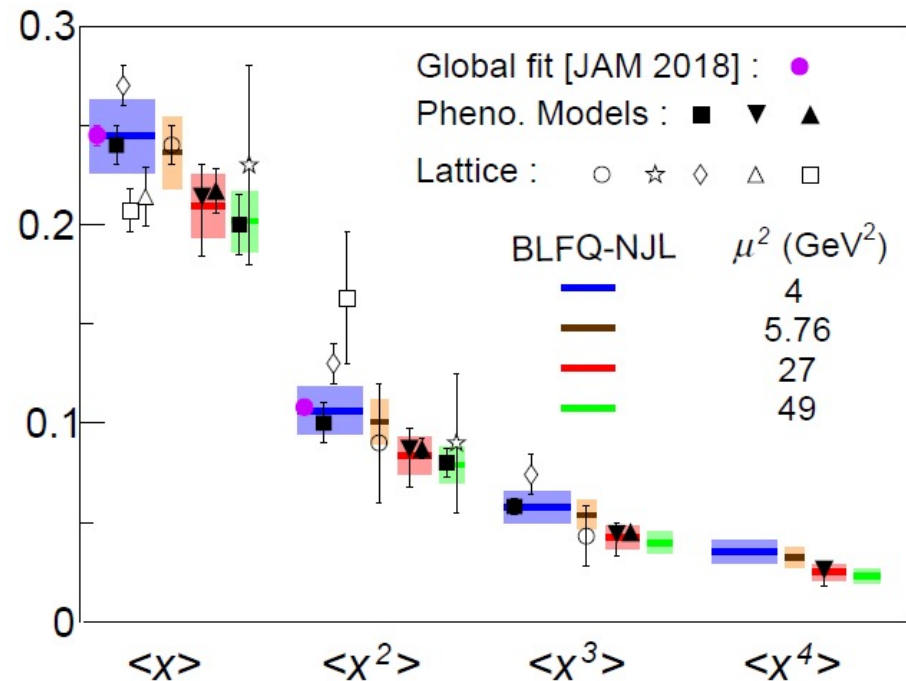


Valence u PDF Kaon/Pion



The Moments of Pion Valence Quark PDF

$$\langle x^n \rangle = \int_0^1 dx x^n f_v^{\pi/K}(x, \mu^2), \quad n = 1, 2, 3, 4.$$



$\langle x \rangle @ 4 \text{ GeV}^2$	Valence	Gluon	Sea
BLFQ-NJL	0.489	0.398	0.113
[Ding <i>et. al.</i> , BSE model 2019']	0.48(3)	0.41(2)	0.11(2)

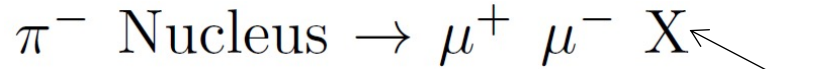
Agree with other results

Drell-Yan Cross Section

[S. D. Drell and T.-M. Yan, PRL (1970)]

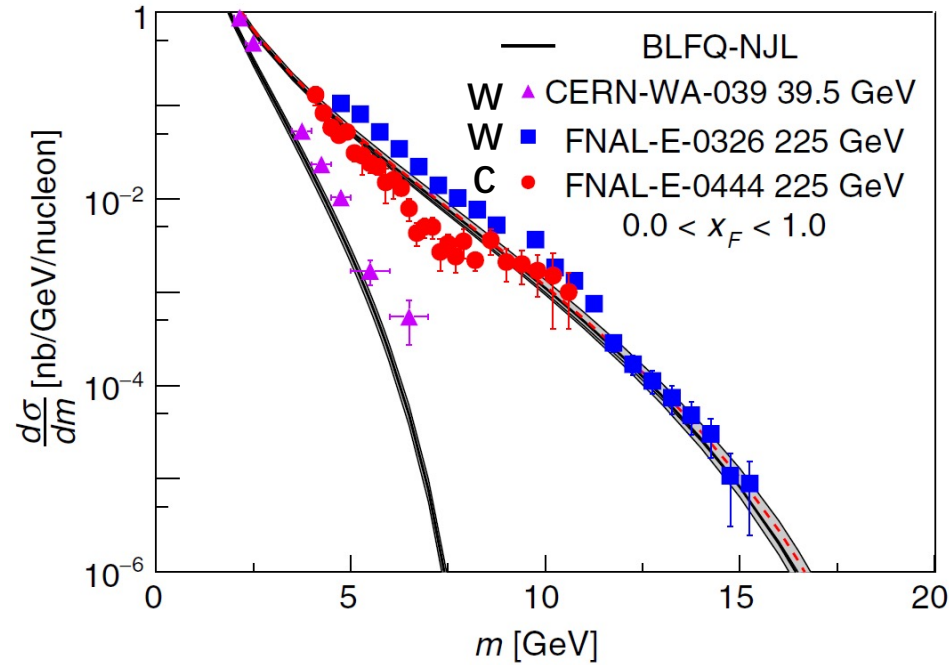
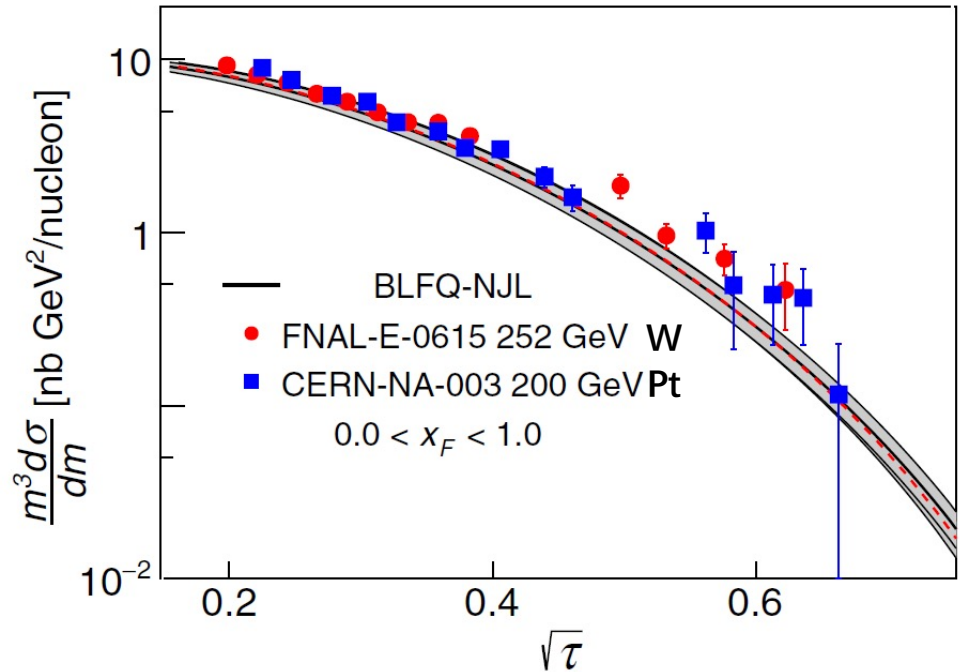
[T. Becher et al, JKEP07(2008)030]; [P. C. Barry et al, PRL121(2018)152001]

[C. Anastasiou et al, PRL91(2003)182002]



[nCTEQ 2015]

$$\frac{m^3 d^2 \sigma}{dmdY} = \frac{8\pi\alpha^2 m^2}{9 s} \sum_{ij} dx_1 dx_2 \tilde{C}_{ij}(x_1, x_2, s, m, \mu_f) f_{i/\pi}(x_1, \mu_f) f_{j/N}(x_2, \mu_f)$$



Agree with experimental data (FNAL E615, 326, 444, & CERN NA3, WA-039).

[Lan, Mondal, Jia, Zhao, Vary, PRD101(2020)034024]

One step forward

[Lan, et al, PRL 19']

$$|\text{meson}\rangle = |q\bar{q}\rangle + \dots$$

[Lan, Fu, Mondal, Zhao, Vary, Phys. Lett. B 825 (2022) 136890]

$$|\text{meson}\rangle = a|q\bar{q}\rangle + b|q\bar{q}g\rangle + \dots$$

H_{int}	$ q\bar{q}\rangle$	$ q\bar{q}g\rangle$
$\langle q\bar{q} $		
$\langle q\bar{q}g $		0

$$H_{\text{eff}} = \frac{\vec{k}_{\perp}^2 + m_q^2}{x} + \frac{\vec{k}_{\perp}^2 + m_{\bar{q}}^2}{1-x} + \kappa^4 x(1-x)\vec{r}_{\perp}^2 - \frac{\kappa^4}{(m_q + m_{\bar{q}})^2} \partial_x(x(1-x)\partial_x) + H_{\text{eff}}^{\text{NJL}}$$



$$P^- = \frac{\vec{k}_{\perp}^2 + m_q^2}{x} + \frac{\vec{k}_{\perp}^2 + m_{\bar{q}}^2}{1-x} + \kappa^4 x(1-x)\vec{r}_{\perp}^2 - \frac{\kappa^4}{(m_q + m_{\bar{q}})^2} \partial_x(x(1-x)\partial_x) + H_{\text{int}}$$

Light-front QCD Hamiltonian

[Brodsky et al, 1998]

$$P_{-,LFQCD} = \frac{1}{2} \int d^3x \bar{\psi} \gamma^+ \frac{(i\partial^\perp)^2 + m^2}{i\partial^+} \psi + \frac{1}{2} \int d^3x A_a^i (i\partial^\perp)^2 A_a^i$$

$$+g \int d^3x \bar{\psi} \gamma_\mu A^\mu \psi$$

$$+ \frac{1}{2} g^2 \int d^3x \bar{\psi} \gamma_\mu A^\mu \frac{\gamma^+}{i\partial^+} \gamma_\nu A^\nu \psi$$

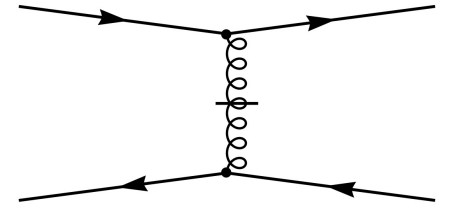
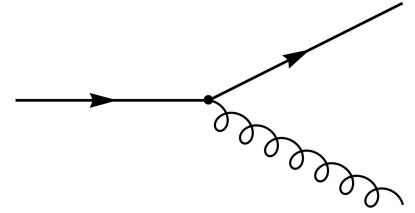
$$-i g^2 \int d^3x f^{abc} \bar{\psi} \gamma^+ T^c \psi \frac{1}{(i\partial^+)^2} (i\partial^+ A_a^\mu A_{\mu b})$$

$$+ \frac{1}{2} g^2 \int d^3x \bar{\psi} \gamma^+ T^a \psi \frac{1}{(i\partial^+)^2} \bar{\psi} \gamma^+ T^a \psi$$

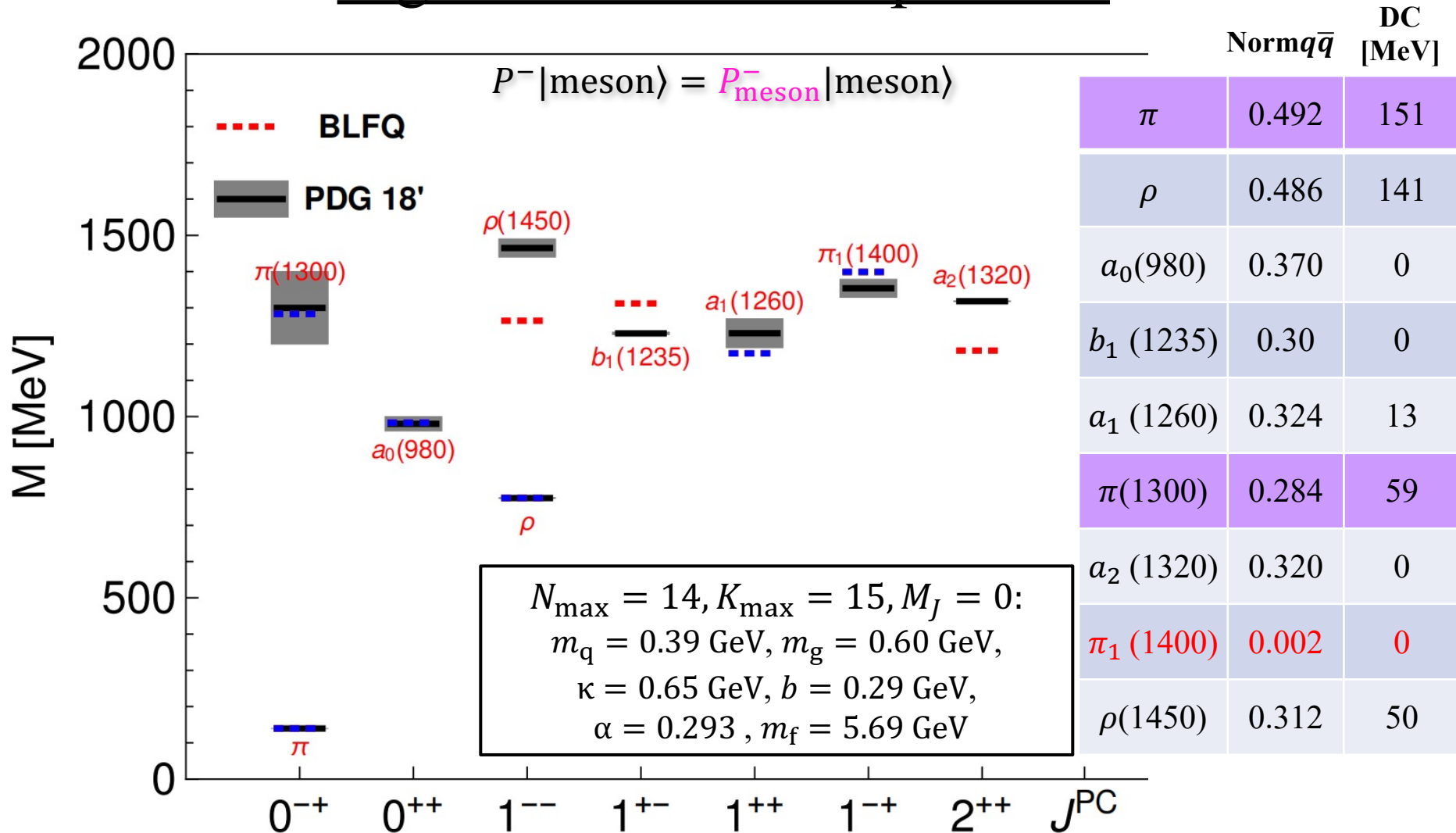
$$+i g \int d^3x f^{abc} i\partial^\mu A^{va} A_\mu^b A_\nu^c$$

$$- \frac{1}{2} g^2 \int d^3x f^{abc} f^{ade} i\partial^+ A_b^\mu A_{\mu c} \frac{1}{(i\partial^+)^2} (i\partial^+ A_d^+ A_{ve})$$

$$+ \frac{1}{4} g^2 \int d^3x f^{abc} f^{ade} A_b^\mu A_c^\nu A_{\mu d} A_{ve}$$



Light Meson Mass Spectrum



$$|\text{meson}\rangle = a|q\bar{q}\rangle + b|q\bar{q}g\rangle + \dots$$

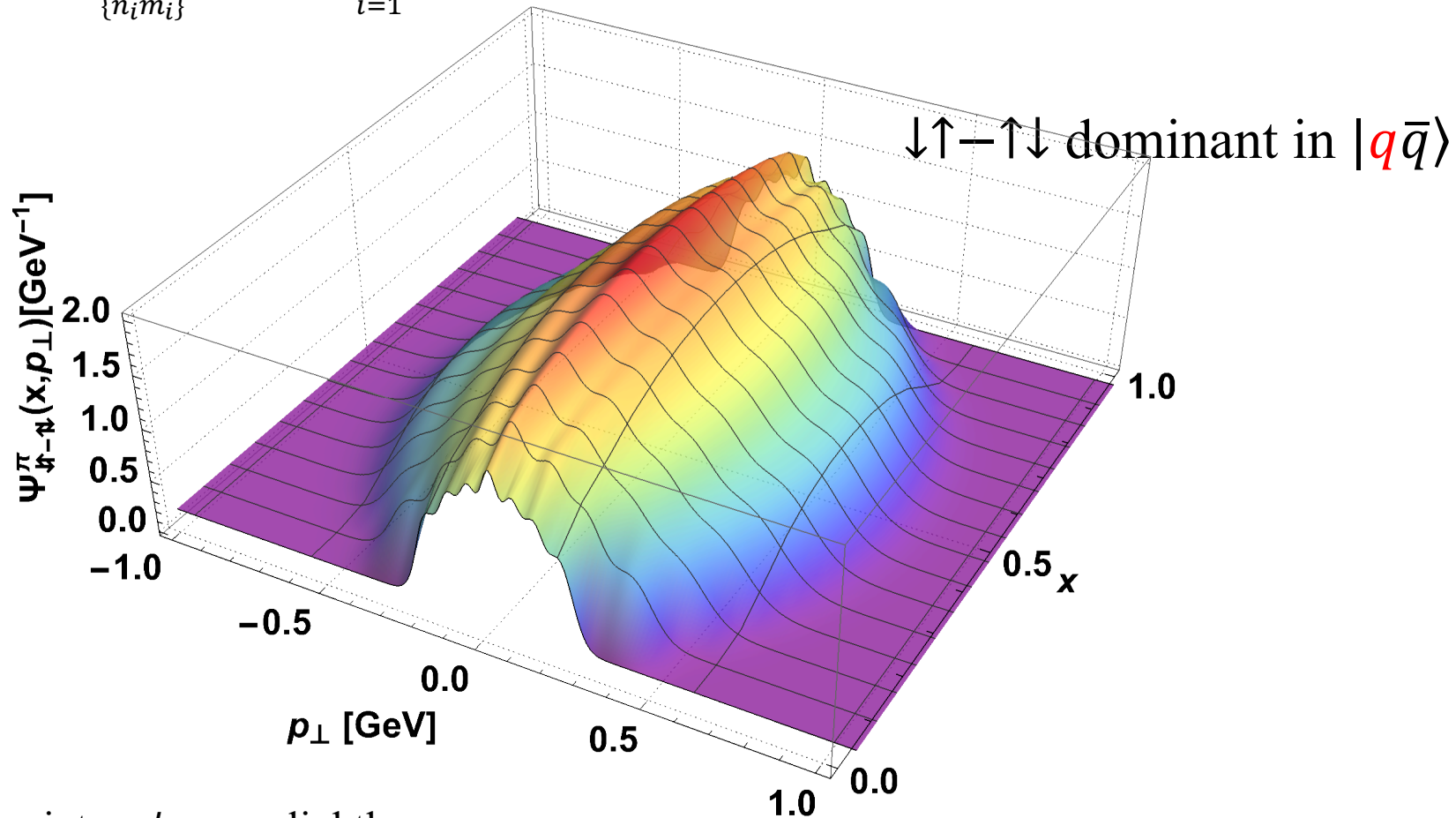
Fix the parameters by fitting six blue states

- $\pi_1(1400)$: $|q\bar{q}g\rangle$ dominates
- $\pi(1300)$: the DC is smaller than the DC of pion

The Wave Function in Leading Fock Sector

$$\Psi_{\{x_i, \vec{p}_{\perp i}, \lambda_i\}}^{\mathcal{N}, M_J} = \sum_{\{n_i m_i\}} \psi^{\mathcal{N}}(\{\bar{\alpha}_i\}) \prod_{i=1}^{\mathcal{N}} \phi_{n_i m_i}(\vec{p}_{\perp i}, b)$$

$$|\pi\rangle = a|q\bar{q}\rangle + b|q\bar{q}g\rangle + \dots$$



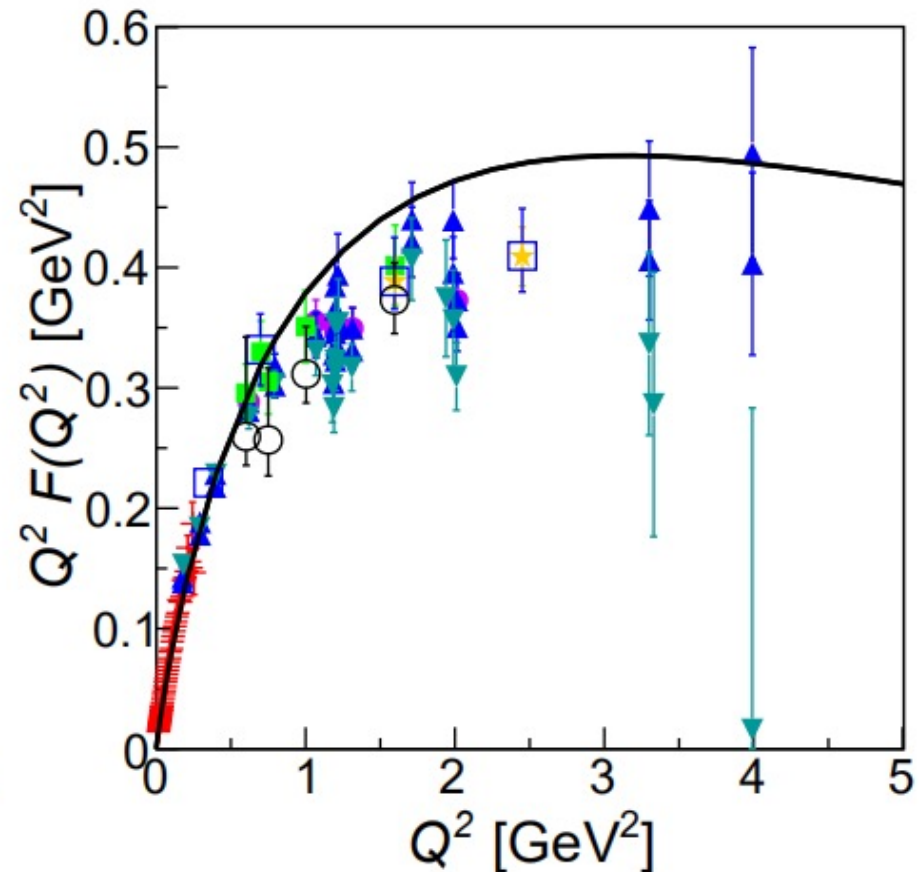
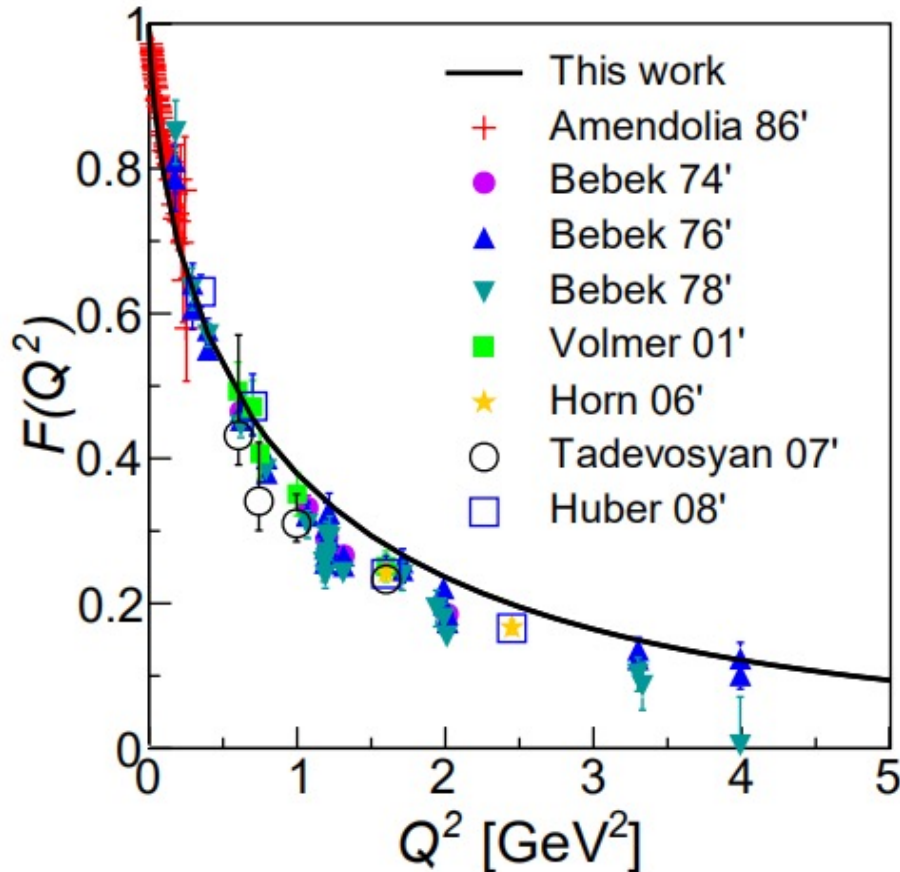
- At endpoint x , $\psi \sim p_{\perp}$: lightly narrow
- At middle x , $\psi \sim p_{\perp}$: a little bit wide

Pion Electromagnetic Form Factor

[Brodsky & de Teramond, PRD 77(2008)056007]

$$|\pi\rangle = a|q\bar{q}\rangle + b|q\bar{q}g\rangle + \dots$$

$$\langle\Psi(p')|J_{EM}^+(0)|\Psi(p)\rangle = (p+p')^+ F(Q^2)$$

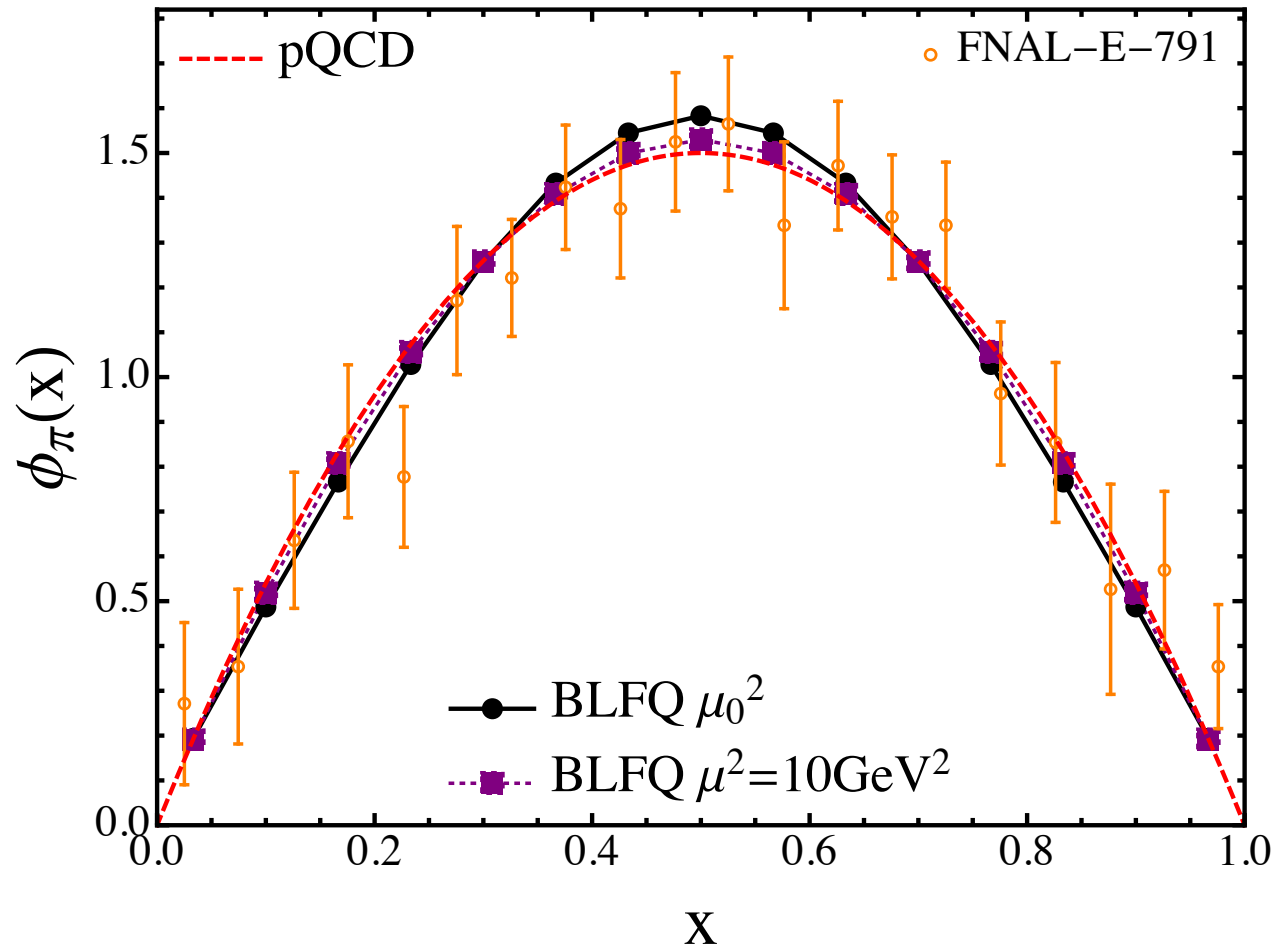


- FF is in reasonable agreement with experimental data
- $F(Q^2) \propto 1/Q^2$ for large Q^2

Pion PDA

$$|\pi\rangle = a|q\bar{q}\rangle + b|q\bar{q}g\rangle + \dots$$

[Ruiz Arriola & Broniowski, PRD 66(2002)094016]

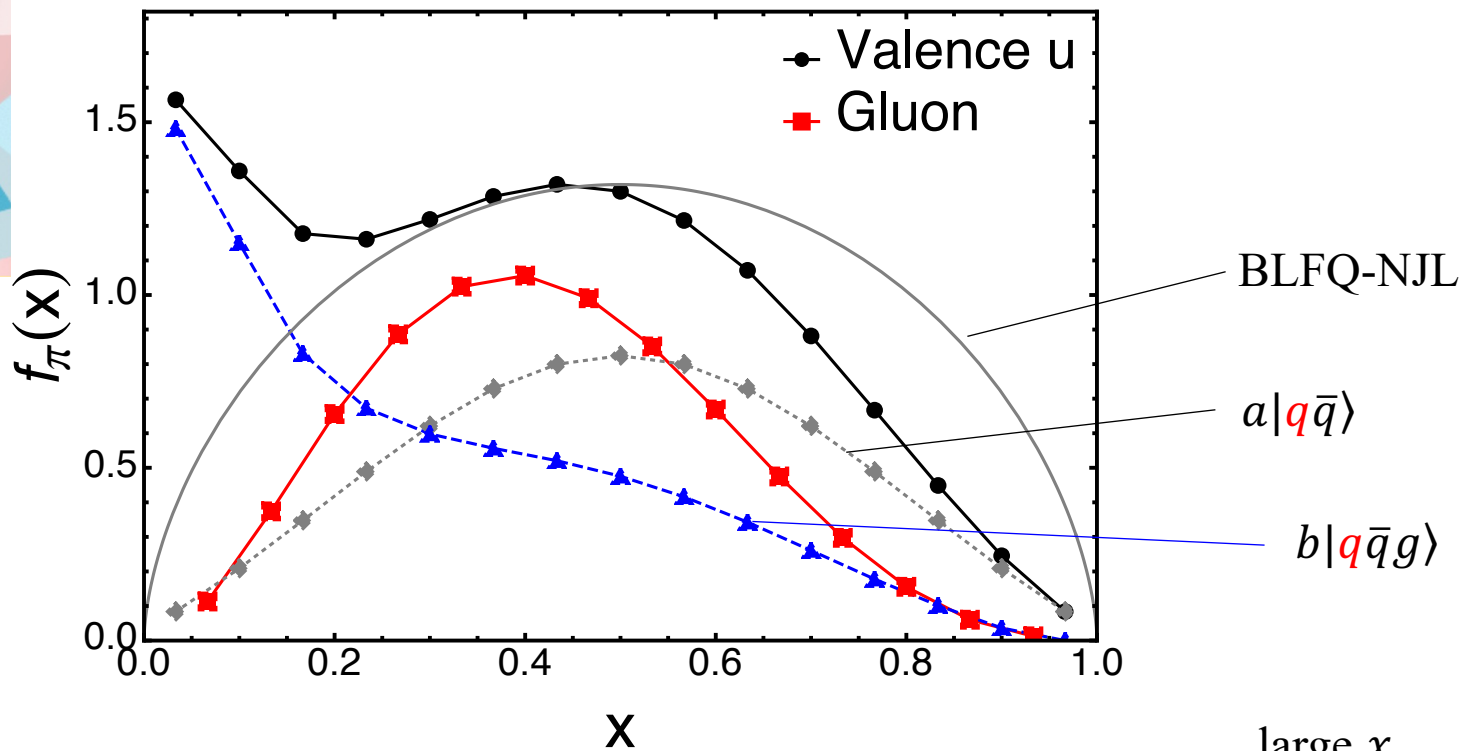


- Endpoint behavior almost agrees with pQCD
- Consistent with FNAL-E-791 experiment

Preliminary

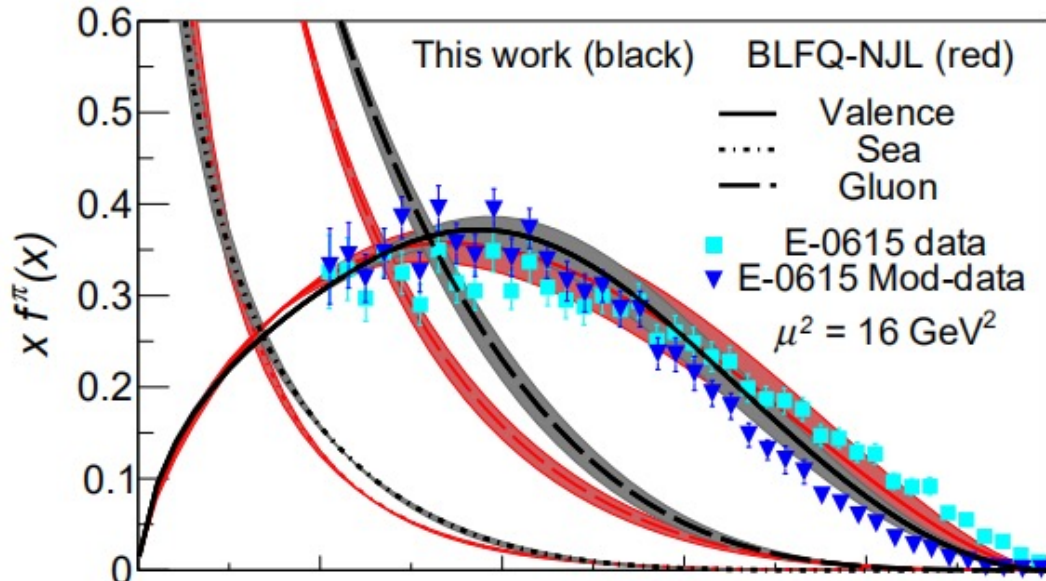
Pion PDF at Model Scale

$$f_i(x) = \sum_{\mathcal{N}, \lambda_i} \int [d\mathcal{X} d\mathcal{P}^\perp]_{\mathcal{N}} \left| \psi_{\{x_i, \vec{p}_{\perp i}, \lambda_i\}}^{\mathcal{N}, M_j=0} \right|^2 \delta(x - x_i) \quad |\pi\rangle = a|q\bar{q}\rangle + b|q\bar{q}g\rangle + \dots$$



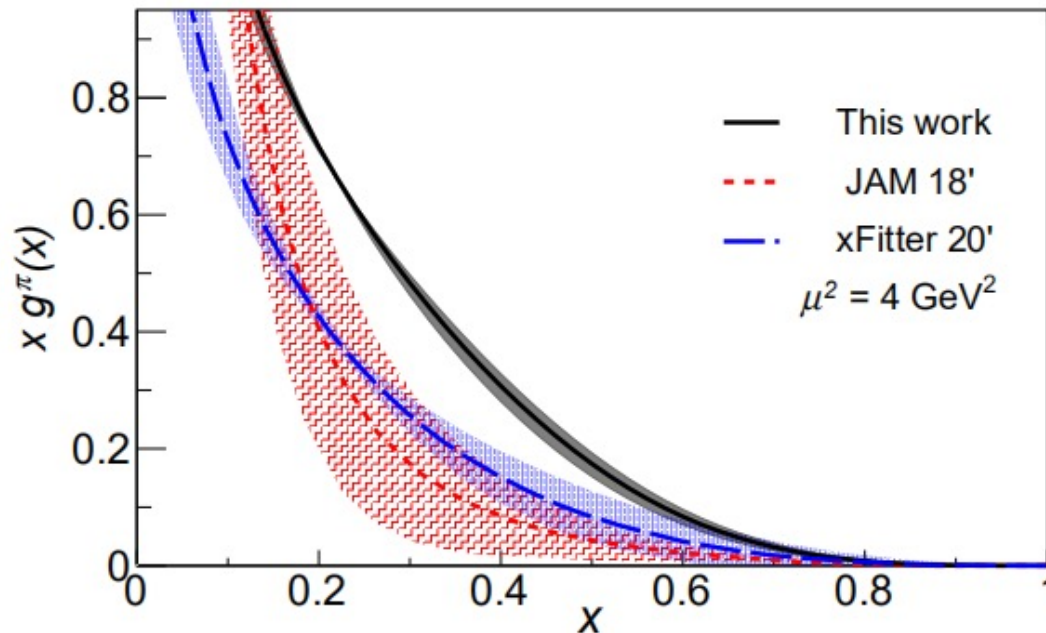
$\mu_{0\text{BLFQ-NJL}}^2 = 0.24 \text{ GeV}^2$	$\langle x \rangle_{\text{gluon}} = 0$;	$\langle x \rangle_{\text{valence } u} = 0.5$	$(1-x)^{0.596}$
$\mu_{0\text{BLFQ}}^2 = 0.34 \text{ GeV}^2$	$\langle x \rangle_{\text{gluon}} = 0.216$;	$\langle x \rangle_{\text{valence } u} = 0.392$	$(1-x)^{1.4}$

Pion PDF with QCD Evolution



$$|\pi\rangle = a|q\bar{q}\rangle + b|q\bar{q}g\rangle + \dots$$

- Large- x behavior $(1-x)^{1.77}$ closer to pQCD
- The gluon distribution significantly increases



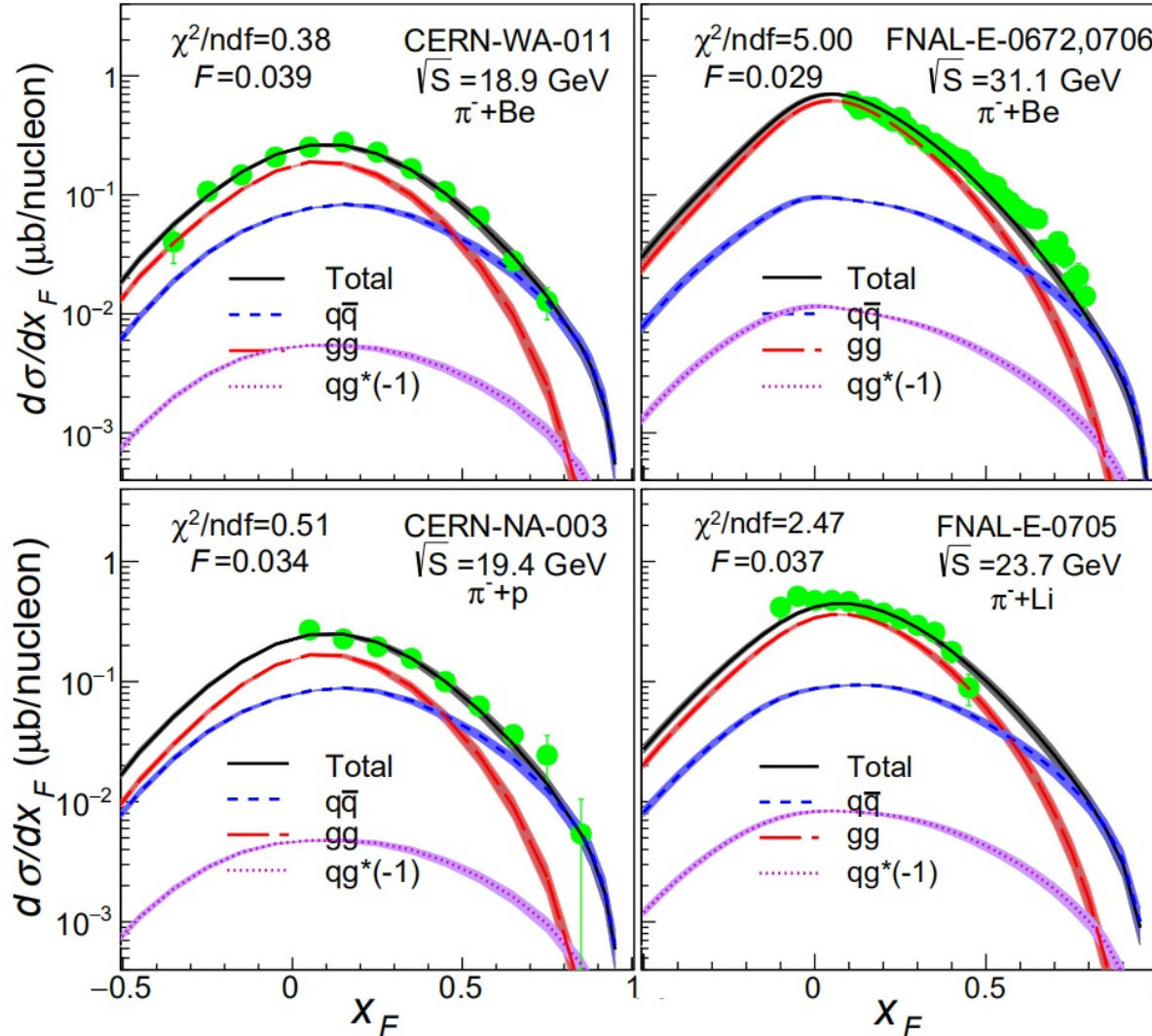
$\langle x \rangle @ 4 \text{ GeV}^2$	Valence	Gluon	Sea
BLFQ	0.483	0.421	0.096
BLFQ-NJL	0.489	0.398	0.113
[BSE 2019']	0.48(3)	0.41(2)	0.11(2)

J/ψ production cross section

$$\pi^\pm N \rightarrow J/\psi X$$

$$\frac{d\sigma}{dx_F} |J/\psi = F \sum_{i,j=q,\bar{q},g} \int_{2m_c}^{2m_D} dM_{c\bar{c}} \frac{2M_{c\bar{c}}}{S \sqrt{x_F^2 + \frac{4M_{c\bar{c}}^2}{S}}} \hat{\sigma}_{ij}(s, m_c^2, \mu_R^2, \mu_F^2) f_i^{\pi^\pm}(x_1, \mu_F^2) f_j^N(x_2, \mu_F^2)$$

[nCTEQ 2015]



CEM

[Chang, et al, PRD 102 (2020) 054024];
 [Nason, et al, NPB 303 (1988) 607];
 [Mangano, et al, NPB 405 (1993) 507]

- significantly gg contribution
- various energies of pions
- different target

Agree with experimental data (FNAL E672, E706, E705, CERN NA3, WA11).

The pion $q\bar{q}g$ BLFQ .vs. BSE

BLFQ

Phys. Lett. B 825 (2022) 136890

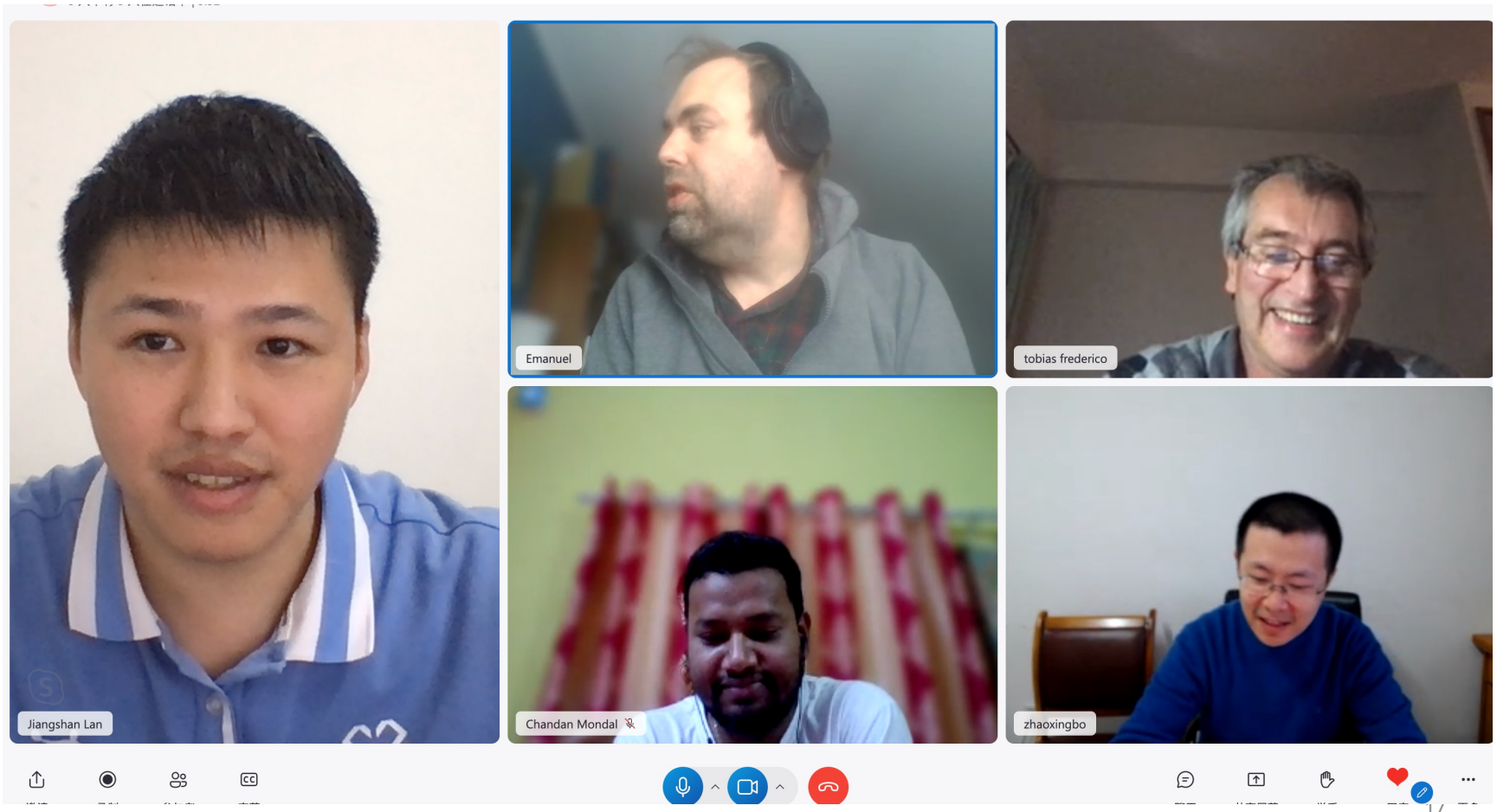
$$|\pi\rangle = a|q\bar{q}\rangle + b|q\bar{q}g\rangle + \dots$$

BSE in Minkowski space

Phys. Rev. D 103 (2021) 014002

Phys. Rev. D 105 (2022) L071505

Phys. Lett. B 820 (2021) 136494



The pion $q\bar{q}g$ BLFQ .vs. BSE

$$P^- P^+ |\Psi\rangle = M^2 |\Psi\rangle$$

$$|\pi\rangle = a|q\bar{q}\rangle + b|q\bar{q}g\rangle + \dots$$

$$\begin{aligned} |\Psi\rangle = & \sum_{i_q s_q} \sum_{i_{\bar{q}} s_{\bar{q}}} \int \left[\prod_{j=q,\bar{q}} \frac{d^3 p_j}{(2\pi)^3 2p_j^+} \right] 2P^+ (2\pi)^3 \delta^3(\mathbf{p}_q + \mathbf{p}_{\bar{q}} - \mathbf{P}) \psi_{q\bar{q},i_q i_{\bar{q}}}^{s_q s_{\bar{q}}} (x_q, \mathbf{p}_{q\perp}, x_{\bar{q}}, \mathbf{p}_{\bar{q}\perp}) b_{i_q s_q}^\dagger(\mathbf{p}_q) d_{i_{\bar{q}} s_{\bar{q}}}^\dagger(\mathbf{p}_{\bar{q}}) |0\rangle \\ & + \sum_{i_q s_q} \sum_{i_{\bar{q}} s_{\bar{q}}} \sum_{\lambda a} \int \left[\prod_{j=q,\bar{q},g} \frac{d^3 p_j}{(2\pi)^3 2p_j^+} \right] 2P^+ (2\pi)^3 \delta^3(\mathbf{p}_q + \mathbf{p}_{\bar{q}} + \mathbf{p}_g - \mathbf{P}) \\ & \times \psi_{q\bar{q}g,i_q i_{\bar{q}} a}^{s_q s_{\bar{q}} \lambda} (x_q, \mathbf{p}_{q\perp}, x_{\bar{q}}, \mathbf{p}_{\bar{q}\perp}, x_g, \mathbf{p}_{g\perp}) b_{i_q s_q}^\dagger(\mathbf{p}_q) d_{i_{\bar{q}} s_{\bar{q}}}^\dagger(\mathbf{p}_{\bar{q}}) a_{\lambda a}^\dagger(\mathbf{p}_g) |0\rangle \\ & + \dots \end{aligned}$$



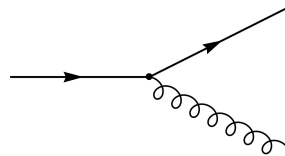
$$|\pi\rangle = a|q\bar{q}\rangle + b|q\bar{q}g\rangle$$

$$\psi_{q\bar{q}g,i_q i_{\bar{q}} a}^{s_q s_{\bar{q}} \lambda} = \frac{1}{M_\pi^2 - M_{0,q\bar{q}g}^2} [V \psi_{q\bar{q},i_q i_{\bar{q}}}^{s_q s_{\bar{q}}}]$$

V : the interaction connecting the $q\bar{q}$ and $q\bar{q}g$ sector

$$\begin{aligned} [V \psi_{q\bar{q},i_q i_{\bar{q}}}^{s_q s_{\bar{q}}}] = & \frac{g_s \sqrt{2}}{x_q + x_{\bar{q}}} \sum_{i_1 s_1} T_{i_q, i_1}^a W_\lambda^{s_q s_1}(p_q, p_g) \psi_{q\bar{q},i_1 i_{\bar{q}}}^{s_1 s_{\bar{q}}}(x_{\bar{q}}, \mathbf{p}_{\bar{q}\perp}) \\ & - \frac{g_s \sqrt{2}}{x_{\bar{q}} + x_g} \sum_{i_1 s_1} T_{i_1, i_{\bar{q}}}^a \bar{W}_\lambda^{s_1 s_q}(p_{\bar{q}}, p_g) \psi_{q\bar{q},i_q i_1}^{s_q s_1}(x_q, \mathbf{p}_{q\perp}) \end{aligned}$$

$$M_{0,q\bar{q}g}^2 = \sum_{j=q\bar{q}g} \frac{\mathbf{p}_{j\perp}^2 + m_j^2}{x_j}$$



$$\mathbf{p}_{q\perp} + \mathbf{p}_{\bar{q}\perp} + \mathbf{p}_{g\perp} = 0, \quad x_q + x_{\bar{q}} + x_g = 1$$

For clarity, we write the spin-flip matrix elements:

[Brodsky et al. Phys. Rep. 301 (1998) 299–486]

$$\begin{aligned} W_\lambda^{+-}(p_q, p_g) &= m_f \frac{x_g(1-x_q)}{\sqrt{x_1 x_q}} \delta_{\lambda,-} \\ W_\lambda^{-+}(p_q, p_g) &= -m_f \frac{x_g(1-x_q)}{\sqrt{x_1 x_q}} \delta_{\lambda,+} \\ \bar{W}_\lambda^{+-}(p_{\bar{q}}, p_g) &= \lambda m_f \frac{x_g(1-x_{\bar{q}})}{\sqrt{x_1 x_{\bar{q}}}} \\ \bar{W}_\lambda^{-+}(p_{\bar{q}}, p_g) &= 0 \end{aligned}$$

The pion $q\bar{q}g$ BLFQ .vs. BSE

The contribution from $q\bar{q}g$ sector to the quark and the gluon PDF:

$$\Delta u_q(x_q) = \frac{1}{(2\pi)^6} \sum_{i_q s_q} \sum_{i_{\bar{q}} s_{\bar{q}}} \sum_{\lambda a} \int \frac{d^2 \mathbf{p}_{q\perp} d^2 \mathbf{p}_{g\perp} dx_g}{4x_q x_g (1-x_q-x_g)} \left| \psi_{q\bar{q}g, i_q i_{\bar{q}} a}^{s_q s_{\bar{q}} \lambda}(x_q, \mathbf{p}_{q\perp}, x_{\bar{q}}, \mathbf{p}_{\bar{q}\perp}, x_g, \mathbf{p}_{g\perp}) \right|^2$$

$$\Delta u_g(x_g) = \frac{1}{(2\pi)^6} \sum_{i_q s_q} \sum_{i_{\bar{q}} s_{\bar{q}}} \sum_{\lambda a} \int \frac{d^2 \mathbf{p}_{q\perp} d^2 \mathbf{p}_{g\perp} dx_q}{4x_q x_g (1-x_q-x_g)} \left| \psi_{q\bar{q}g, i_q i_{\bar{q}} a}^{s_q s_{\bar{q}} \lambda}(x_q, \mathbf{p}_{q\perp}, x_{\bar{q}}, \mathbf{p}_{\bar{q}\perp}, x_g, \mathbf{p}_{g\perp}) \right|^2$$

[Phys. Rev. D 50 (1994) 6895]

Take a power-law form for simplicity:

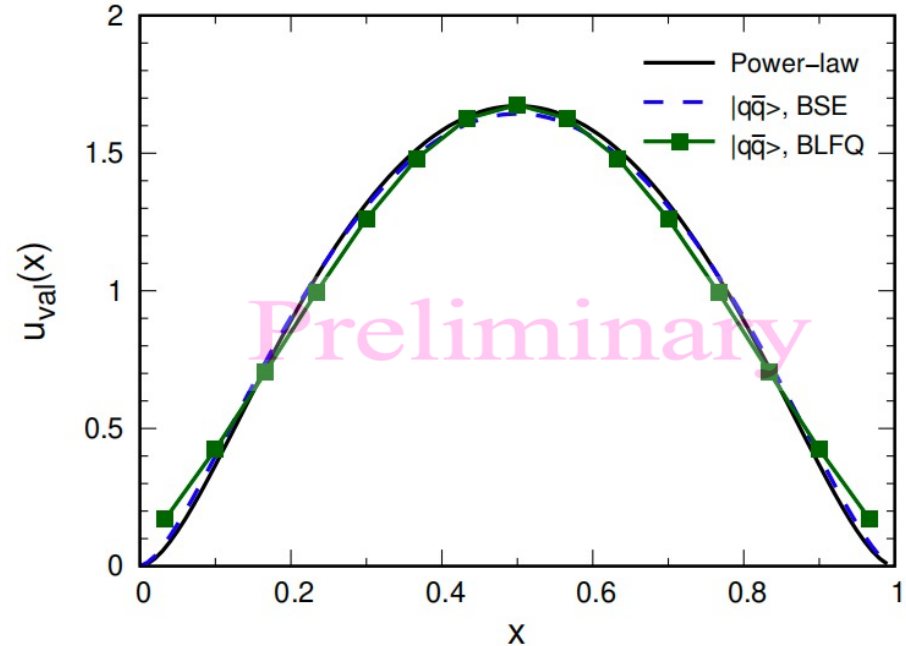
$$\psi_{pl}(x_q, \mathbf{p}_{q\perp}) = N \left[1 + \frac{A_{0,eff}(x_q, \mathbf{p}_{q\perp})/4 - m_q^2}{\beta^2} \right]^{-s}$$

$$A_{0,eff}(x_q, \mathbf{p}_{q\perp}) = \frac{\mathbf{p}_{q\perp}^2 + m_q^2}{x_q} + \frac{\mathbf{p}_{\bar{q}\perp}^2 + m_{\bar{q}}^2}{x_{\bar{q}}}$$

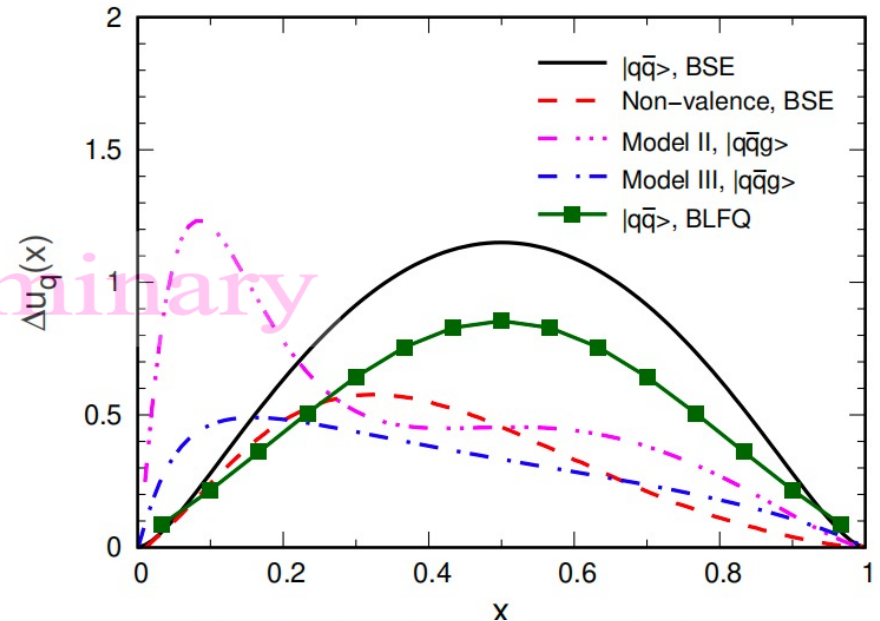
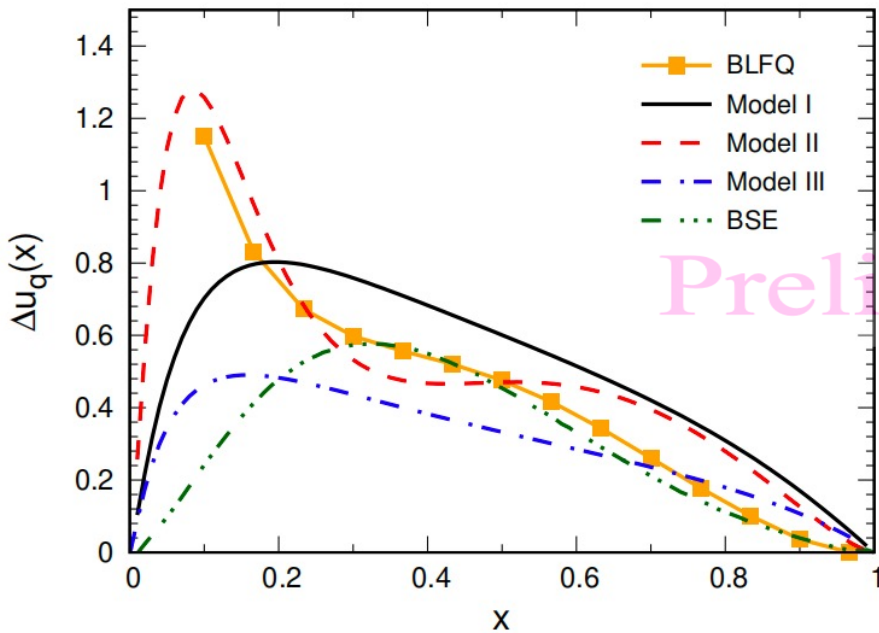
Fitting the valence PDF of both the BLFQ and the BSE, $s = 1.4$ and $\beta/m_q = 1.16$

BLFQ: Phys. Lett. B 825 (2022) 136890

BSE: Phys. Rev. D 103 (2021) 014002



The pion $q\bar{q}g$ BLFQ .vs. BSE



BLFQ: [Phys. Lett. B 825 \(2022\) 136890](#)

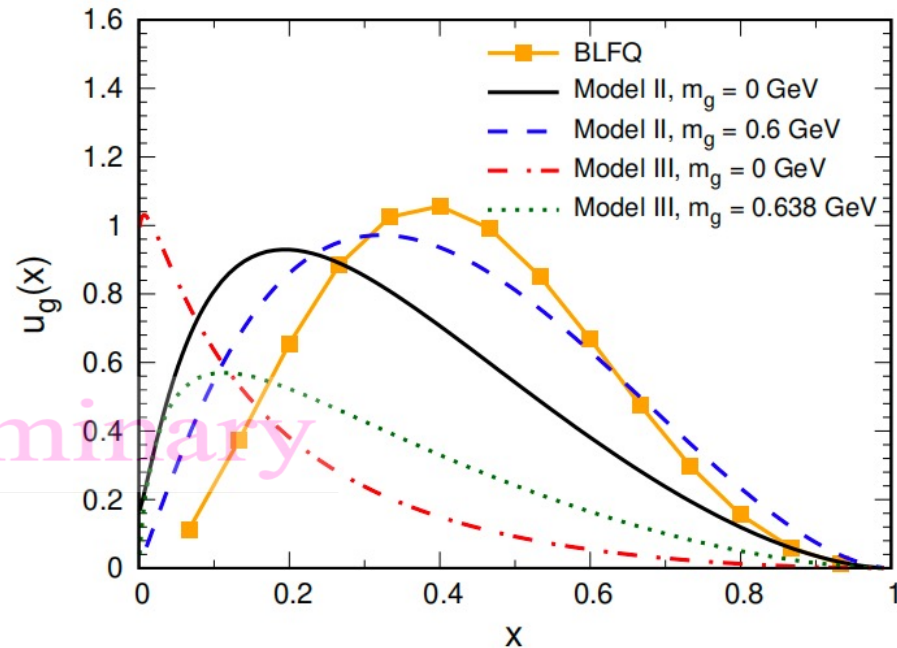
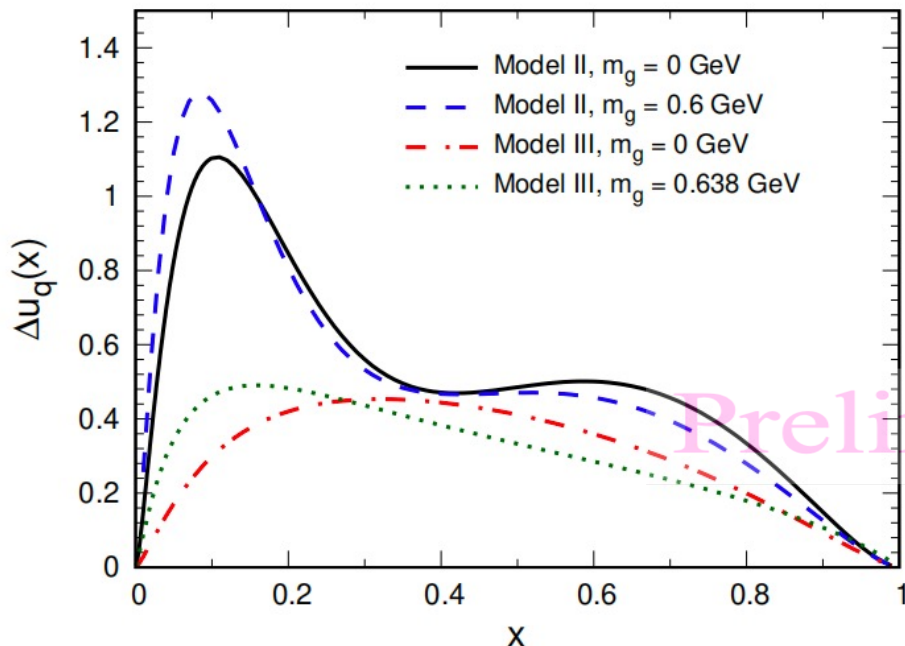
BSE: [Phys. Rev. D 103 \(2021\) 014002](#)

- BLFQ \sim discrete x .vs. Model \sim continuous x
- The Model II agrees with the BLFQ: a large bump at low- x is reproduced
- Model I .vs. II: the bump is related to the large value of m_f
- The BSE result differs from Model III: the BSE result contains the contributions from $q\bar{q}ng$, where $n = 1, 2, \dots, \infty$
- The second Fock sector is mostly important at small- x

Table 1: Quark mass in kinetic part of Hamiltonian, quark mass in one-gluon-exchange interaction and gluon mass for the three adopted parameter sets in GeV. In the rightmost column is displayed the used probability of the $q\bar{q}g$ component.

Model	m_q [GeV]	m_f [GeV]	m_g [GeV]	$1-P_{val}$
I	0.390	0.390	0.600	0.508
II	0.390	5.69	0.600	0.508
III	0.255	0.255	0.638	0.300

The pion $q\bar{q}g$ BLFQ .vs. BSE



BLFQ: *Phys. Lett. B* 825 (2022) 136890
 BSE: *Phys. Rev. D* 103 (2021) 014002

Table 1: Quark mass in kinetic part of Hamiltonian, quark mass in one-gluon-exchange interaction and gluon mass for the three adopted parameter sets in GeV. In the rightmost column is displayed the used probability of the $q\bar{q}g$ component.

Model	m_q [GeV]	m_f [GeV]	m_g [GeV]	$1-P_{val}$
I	0.390	0.390	0.600	0.508
II	0.390	5.69	0.600	0.508
III	0.255	0.255	0.638	0.300

The impact of the m_g on the pion PDFs:

- An increase of the m_g leads to a shift of the quark PDF to lower values of x
- A larger m_g gives a gluon PDF shifted towards larger- x
- The perturbative results agree qualitatively with the BLFQ

The pion $q\bar{q}g$ BLFQ .vs. BSE

We explicitly show an enhancement of the low-x contribution in the quark PDF is directly associated with the large spin-flip matrix element, necessary to provide the $\pi - \rho$ mass splitting.

[M. Burkardt, *Dynamical vertex mass generation and chiral symmetry breaking on the light front*, Phys. Rev. D 58 (1998) 096015].

It was proposed to enhance the spin flip matrix element of the effective quark-gluon coupling QCD LF-Hamiltonian by introducing a large effective quark vertex mass (m_f).

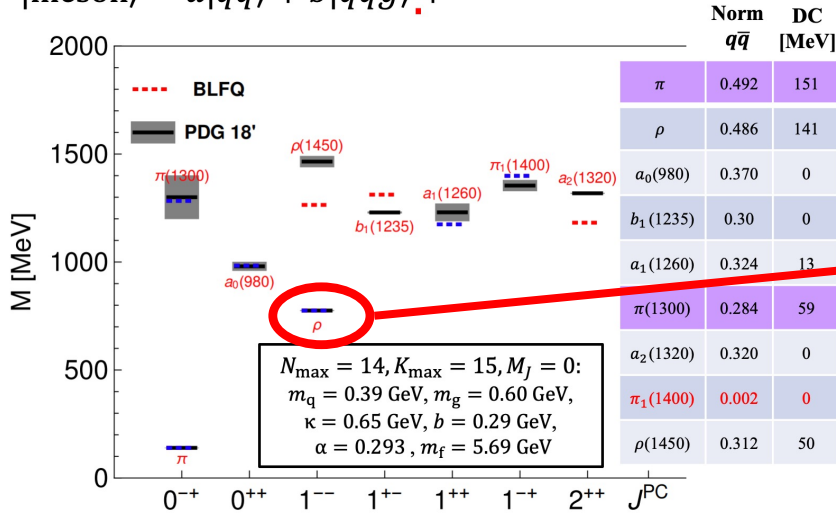
The screenshot shows a Skype meeting interface. The main window displays a plot of $mass^2$ versus m_f . The y-axis ranges from -0.6 to 0.6, and the x-axis ranges from 0 to 6. Two data series are shown: 'pion' (red solid line with circles) and 'rho' (blue dashed line with squares). Both series show a linear increase in $mass^2$ as m_f increases. The pion series starts at approximately -0.55 at $m_f=0$ and reaches about 0.05 at $m_f=6$. The rho series starts at approximately -0.55 at $m_f=0$ and reaches about 0.65 at $m_f=6$. A small diagram in the bottom right corner of the plot area shows a quark line and a gluon line. The Skype interface includes a top bar with the meeting title 'Discussion Xingbo et al', a video gallery with participants Emanuel, Chandan, zhaoxingbo, tobias frederico, and Jiangshan Lan, and a chat window on the right. The chat window shows a message from tobias@ita.br with a file named 'figmf_blfq_plb.pdf' (38.9 KB) and a link to the Light-Cone 2023 conference.

m_f	pion $mass^2$	rho $mass^2$
0	-0.55	-0.55
1	-0.50	-0.45
2	-0.40	-0.30
3	-0.25	-0.10
4	-0.15	0.10
5	-0.05	0.30
6	0.05	0.65

Vector meson Structure



$$|\text{meson}\rangle = a|q\bar{q}\rangle + b|q\bar{q}g\rangle + \dots$$



$N_{\text{max}} = 14, K_{\text{max}} = 15, M_J = 0;$
 $m_q = 0.39 \text{ GeV}, m_g = 0.60 \text{ GeV},$
 $\kappa = 0.65 \text{ GeV}, b = 0.29 \text{ GeV},$
 $\alpha = 0.293, m_f = 5.69 \text{ GeV}$

“Structure of spin-1 QCD systems using light-front Hamiltonian approach”
Satvir Kaur
Thursday 4:30pm-4:50pm

Quark TMDs of a spin-1 target

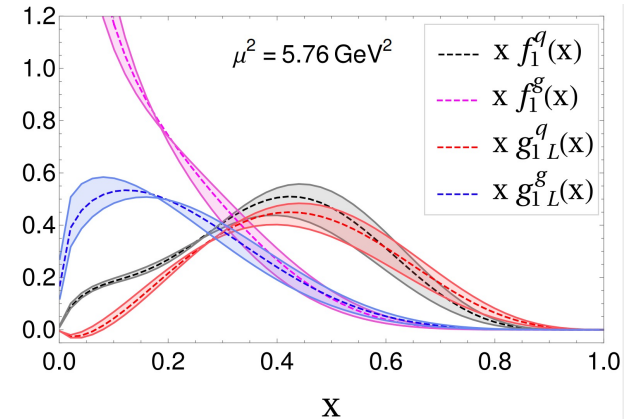
leading twist	quark operator		
	unpolarized [U]	longitudinal [L]	transverse [T]
U	$f_1 = \text{unpolarized}$		$h_1^{\perp} = \text{Boer-Mulders}$
L		$g_1 = \text{helicity}$	$h_{1L}^{\perp} = \text{worm gear 1}$
T	$f_{1T}^{\perp} = \text{Sivers}$	$g_{1T} = \text{worm gear 2}$	$h_1 = \text{transversity}$ $h_{1T}^{\perp} = \text{pretzelosity}$
ROUSENF	$f_{1LL}(x, k_T^2)$ $f_{1LT}(x, k_T^2)$ $f_{1TT}(x, k_T^2)$	$g_{1TT}(x, k_T^2)$ $g_{1LT}(x, k_T^2)$	$h_{1LL}^{\perp}(x, k_T^2)$ $h_{1TT}^{\perp}, h_{1TT}^{\perp}$ $h_{1LT}^{\perp}, h_{1LT}^{\perp}$

Image taken from arXiv: 2205.01249

Gluon TMDs of a spin-1 target

TARGET SPIN	PARTON SPIN		
	GLUONS	$-g_T^{c\beta}$	$\varepsilon_T^{c\beta}$
U	f_1^g		$P_T^{c\beta}, \dots$
L		g_1^g	$h_{1L}^{\perp g}$
T	$f_{1T}^{\perp g}$	g_{1T}^g	$h_1^g, h_{1T}^{\perp g}$
LL	f_{1LL}^g		$h_{1LL}^{\perp g}$
LT	f_{1LT}^g	g_{1LT}^g	$h_{1LT}^g, h_{1LT}^{\perp g}$
TT	f_{1TT}^g	g_{1TT}^g	$h_{1TT}^g, h_{1TT}^{\perp g}, h_{1TT}^{\perp\perp g}$

Picture Credit: P.J. Mulders



Preliminary



Pion TMD

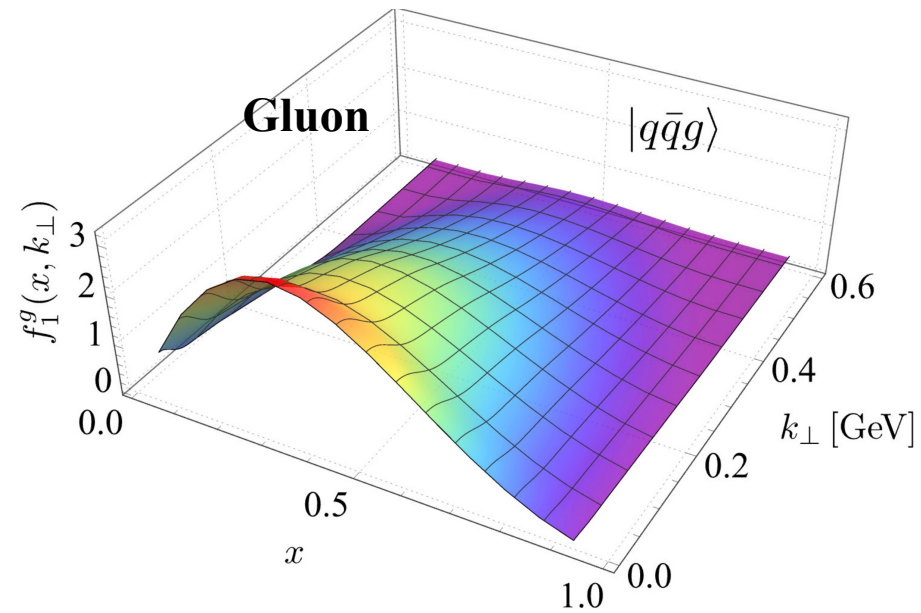
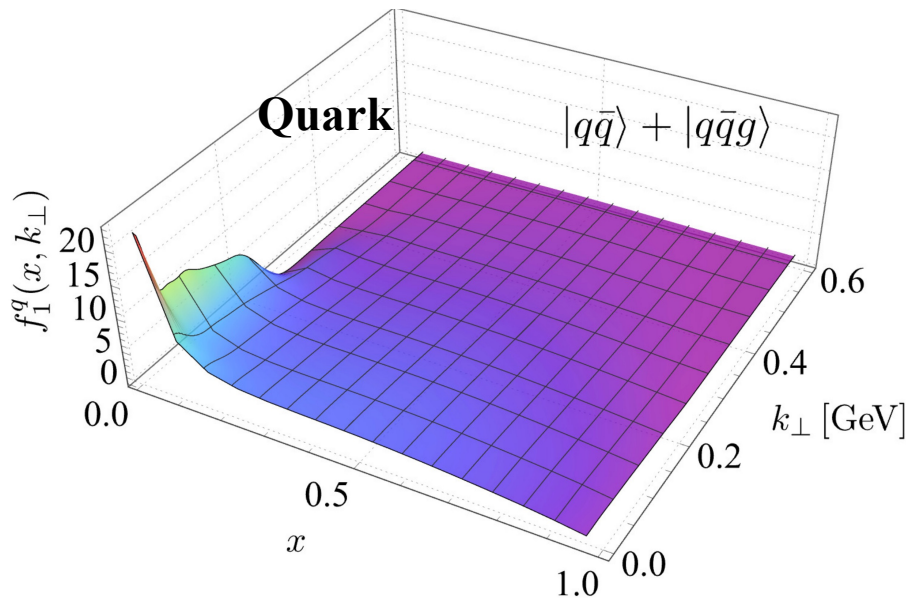
[Boer & Mulders PRD 57 (1998) 5780]

[Pasquini et al, PRD 90 (2014) 014050]

$$|\pi\rangle = a|q\bar{q}\rangle + b|q\bar{q}g\rangle + \dots$$

$$f_1^q(x, k_\perp) = \frac{1}{2} \int \frac{dz^- d^2 z_\perp}{(2\pi)^3} e^{i(z^- k^+ - z_\perp k_\perp)} \left\langle \pi, P \left| \bar{q} \left(-\frac{Z}{2} \right) \gamma^+ q \left(\frac{Z}{2} \right) \right| \pi, P \right\rangle_{z^+=0}$$

$$f_1^g(x, k_\perp) = \frac{1}{xP^+} \int \frac{dz^- d^2 z_\perp}{(2\pi)^3} e^{i(z^- k^+ - z_\perp k_\perp)} \left\langle \pi, P \left| G^{+\mu} \left(-\frac{Z}{2} \right) G_\mu^+ \left(\frac{Z}{2} \right) \right| \pi, P \right\rangle_{z^+=0}$$



- The TMD decreases with k_\perp
- Vanishes after $k_\perp \sim 0.6$ GeV

Preliminary

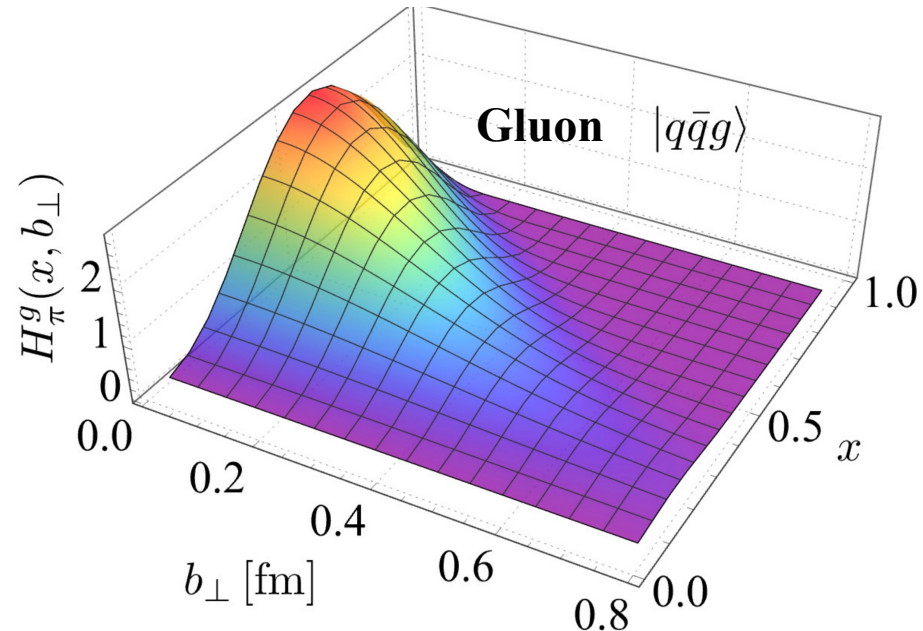
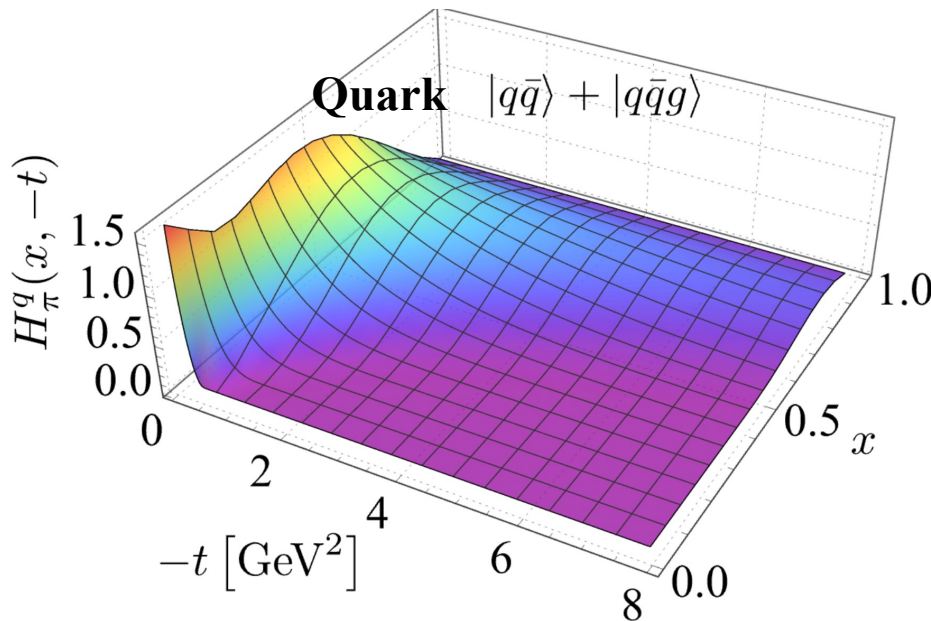
Pion GPD

[M. Diehl, Phys. Rep. 388 (2003) 41-277]

$$|\pi\rangle = a|q\bar{q}\rangle + b|q\bar{q}g\rangle + \dots$$

$$H_{\pi}^q(x, \xi = 0, t) = \frac{1}{2} \int \frac{dz^-}{2\pi} e^{ixP^+z^-} \left\langle \pi, P + \frac{\Delta}{2} \left| \bar{q} \left(-\frac{Z}{2} \right) \gamma^+ q \left(\frac{Z}{2} \right) \right| \pi, P - \frac{\Delta}{2} \right\rangle_{\substack{z^+=0 \\ z_{\perp}=0}}$$

$$H_{\pi}^g(x, \xi = 0, t) = \frac{1}{P^+} \int \frac{dz^-}{2\pi} e^{ixP^+z^-} \left\langle \pi, P + \frac{\Delta}{2} \left| G^{+\mu} \left(-\frac{Z}{2} \right) G_{\mu}^+ \left(\frac{Z}{2} \right) \right| \pi, P - \frac{\Delta}{2} \right\rangle_{\substack{z^+=0 \\ z_{\perp}=0}}$$



- Quark content enhanced at small x with $|q\bar{q}g\rangle$
- Falls slowly at larger x
- Emerge at larger x range for larger $-t$

Preliminary

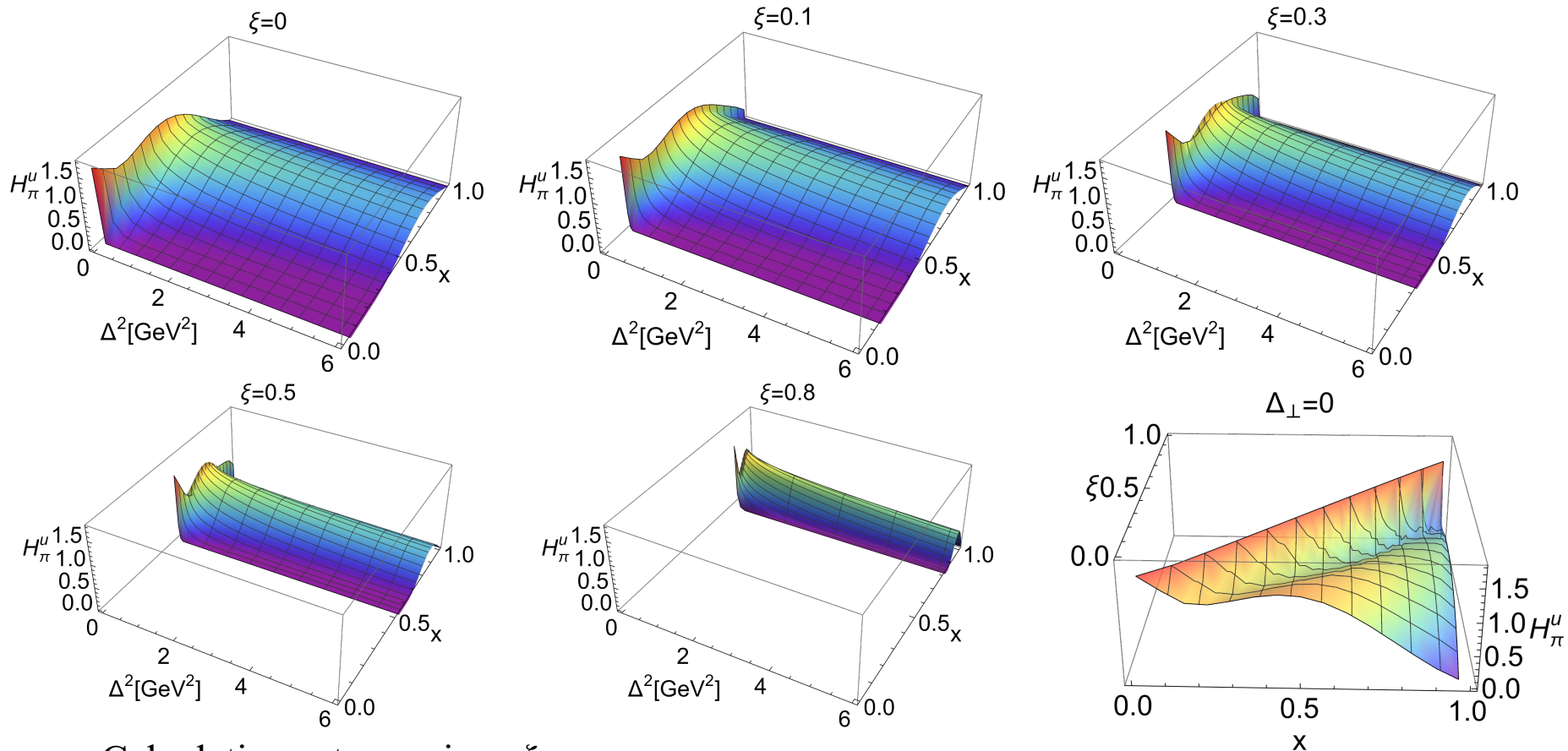
Pion nonzero-skewness GPD



[M. Diehl, Phys. Rep. 388 (2003) 41-277]

$$|\pi\rangle = a|q\bar{q}\rangle + b|q\bar{q}g\rangle + \dots$$

$$H_\pi^q(x, \xi, t) = \frac{1}{2} \int \frac{dz^-}{2\pi} e^{ixP^+z^-} \left\langle \pi, P + \frac{\Delta}{2} \left| \bar{q} \left(-\frac{z}{2} \right) \gamma^+ q \left(\frac{z}{2} \right) \right| \pi, P - \frac{\Delta}{2} \right\rangle_{z^+=0; z_\perp=0}$$



- Calculations at any given ξ
- Emerge at larger x range for larger $-t = \Delta^2$

Preliminary

Light Meson Mass Spectrum



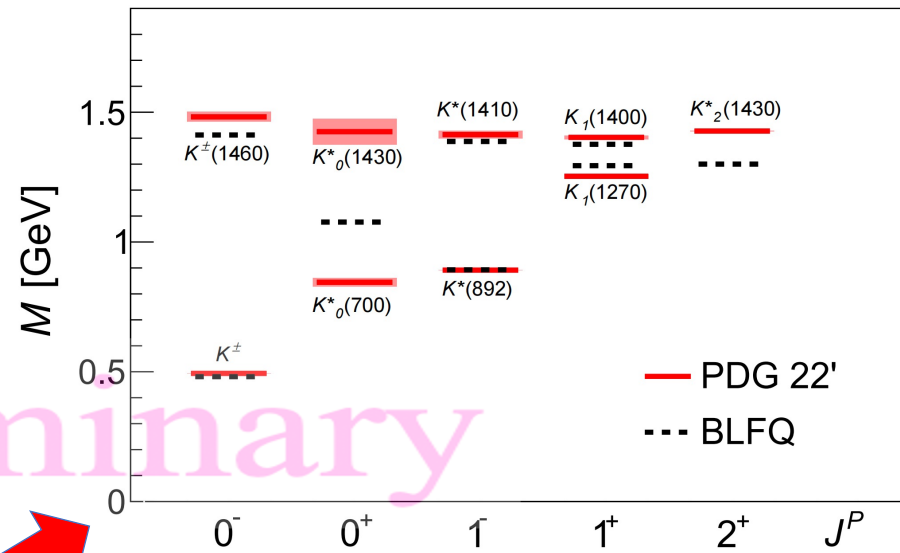
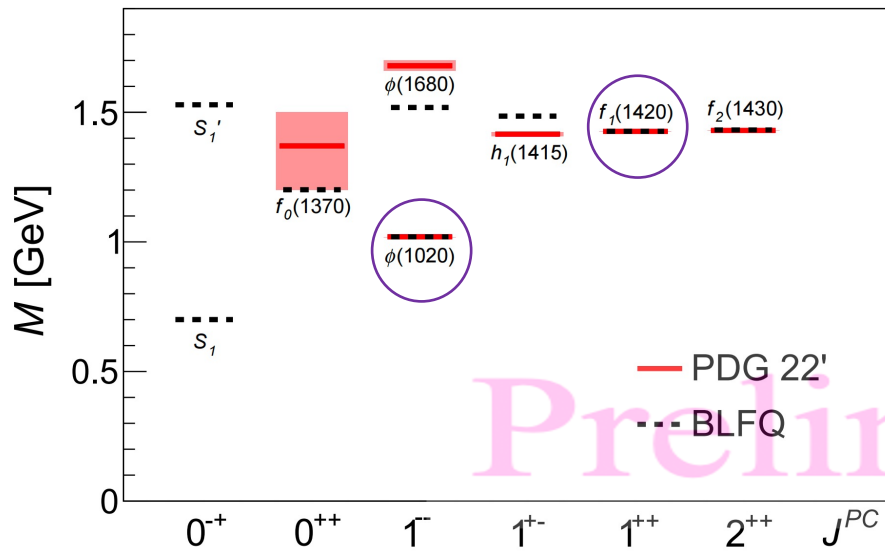
$$P^-|\text{meson}\rangle = P_{\text{meson}}^-|\text{meson}\rangle$$

$$|\text{meson}\rangle = a|q\bar{q}\rangle + b|q\bar{q}g\rangle + \dots$$

[Lan, et al, PLB 825 (2022) 136890]



$$|\text{meson}\rangle = a|s\bar{s}\rangle + b|s\bar{s}g\rangle + \dots \rightarrow |\text{meson}\rangle = a|q\bar{s}\rangle + b|q\bar{s}g\rangle + \dots$$



Preliminary

In units of GeV except g_s [Lan, et al, PLB 22']

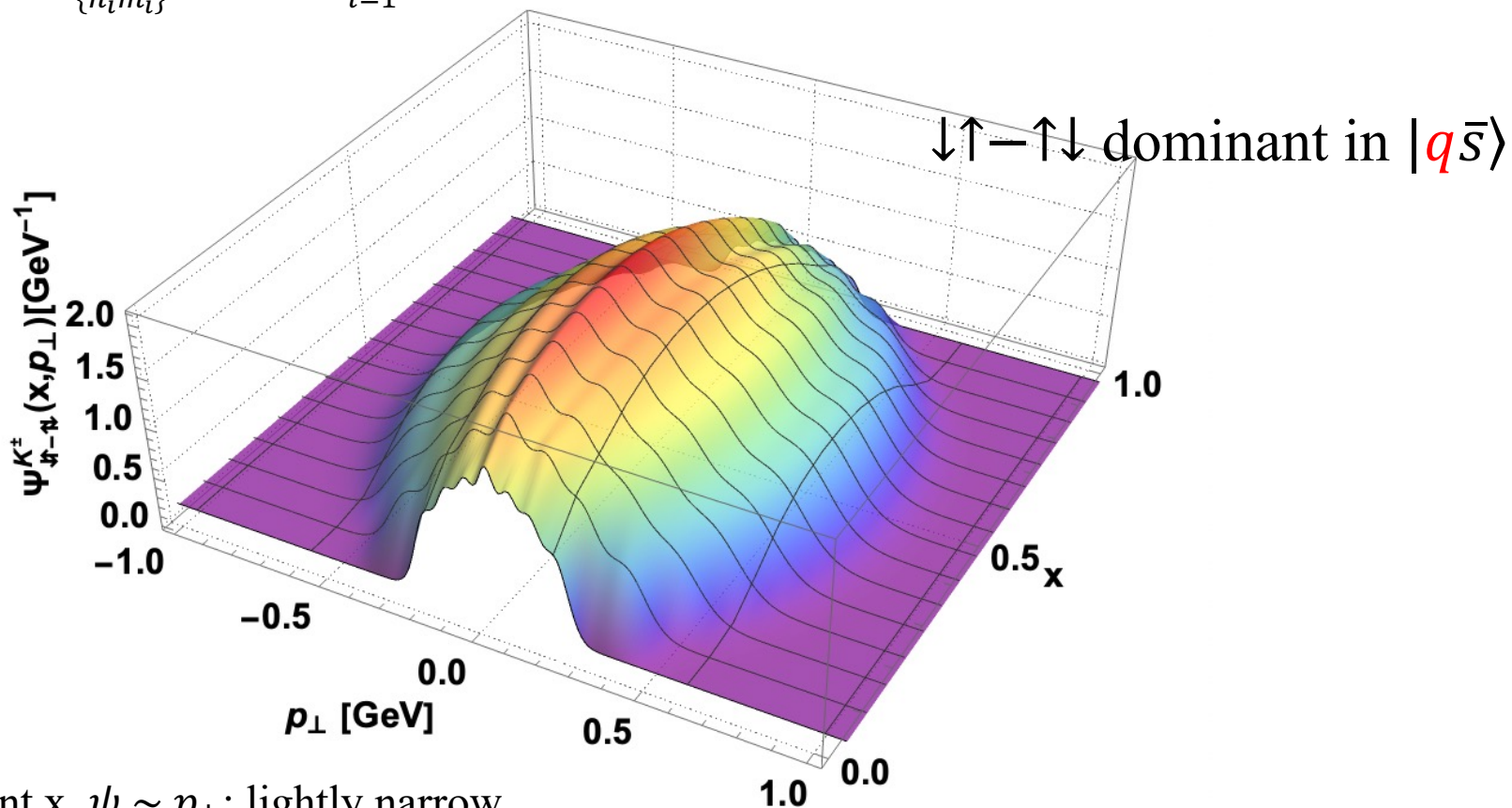
m_q	m_{f_q}	m_g	b	κ	g_s	m_s	m_{f_s}
0.39	5.69	0.60	0.29	0.65	1.92	0.55	7.13

- Agree with experimental data (K , $K^*(892)$, $K^*(1410)$, $K_1(1270)$, $K_1(1400)$)
- The DC of kaon, 156.9 MeV, agrees with the result from the PDG 18', 155.6(4) MeV

The Wave Function in Leading Fock Sector

$$\Psi_{\{x_i, \vec{p}_{\perp i}, \lambda_i\}}^{\mathcal{N}, M_J} = \sum_{\{n_i m_i\}} \psi^{\mathcal{N}}(\{\bar{\alpha}_i\}) \prod_{i=1}^{\mathcal{N}} \phi_{n_i m_i}(\vec{p}_{\perp i}, b)$$

$$|K\rangle = a|q\bar{s}\rangle + b|q\bar{s}g\rangle + \dots$$



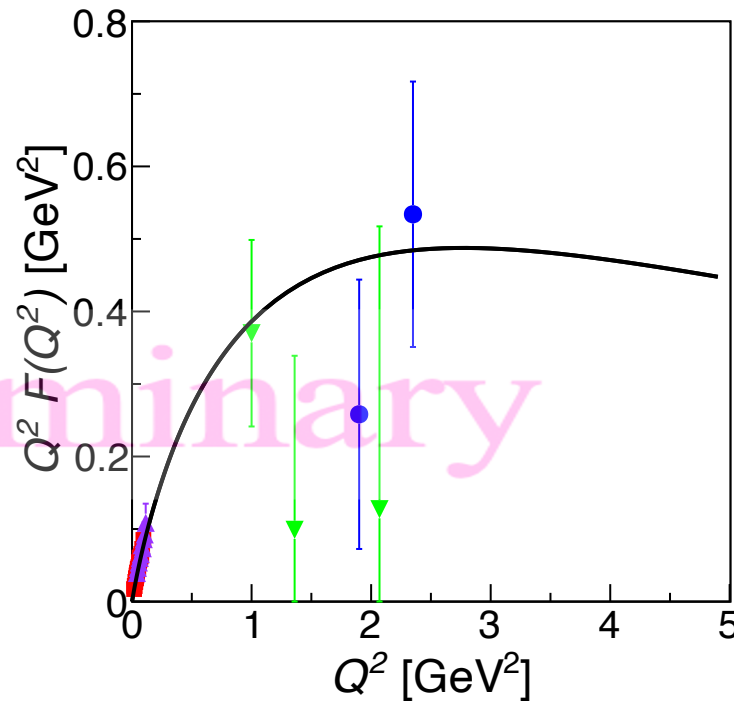
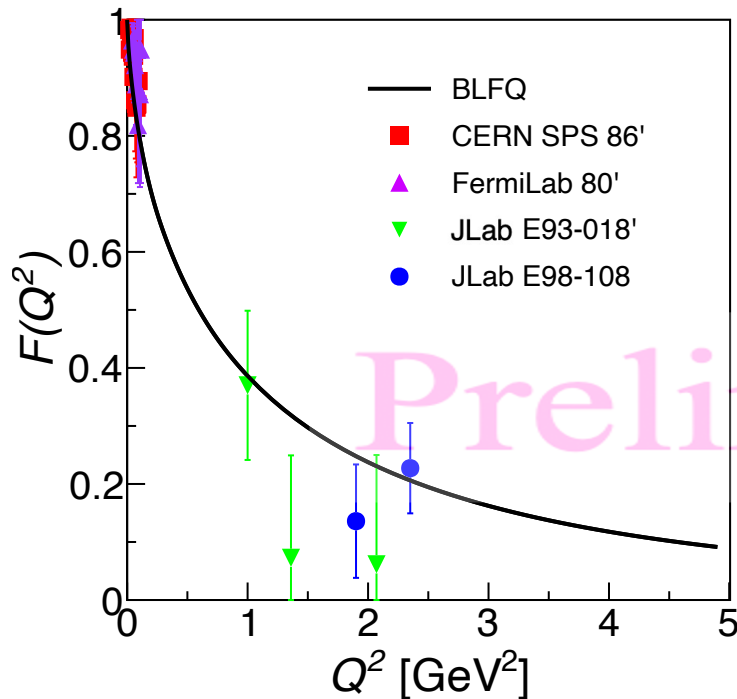
- At endpoint x , $\psi \sim p_{\perp}$: lightly narrow
- At middle x , $\psi \sim p_{\perp}$: a little bit wide
- The peak slightly less than $x=1/2$

Kaon Electromagnetic Form Factor

[Brodsky & de Teramond, PRD 77:056007 (2008)]

$$\langle \Psi(p') | J_{EM}^+(0) | \Psi(p) \rangle = (p + p')^+ F(Q^2)$$

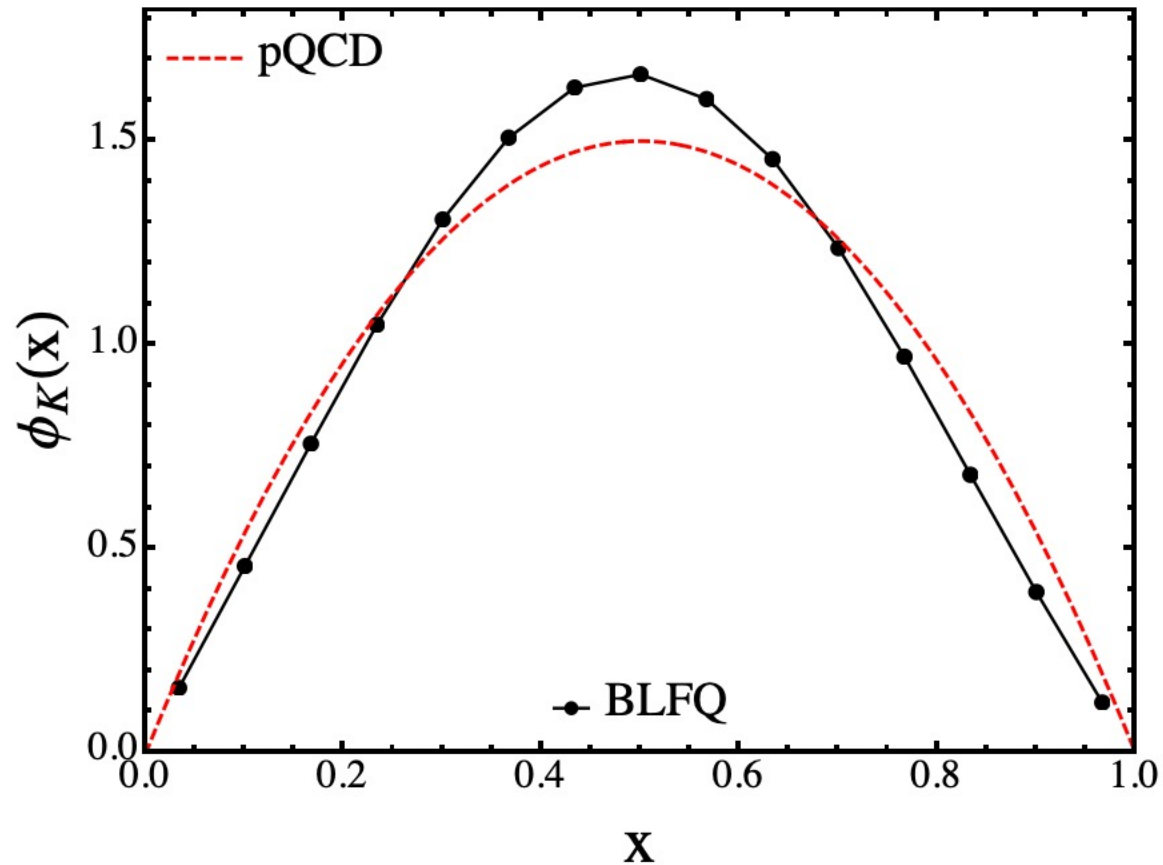
$$|K\rangle = a|q\bar{s}\rangle + b|q\bar{s}g\rangle + \dots$$



- FF is in reasonable agreement with experimental data
- $F(Q^2) \propto 1/Q^2$ for large Q^2

Kaon PDA

$$|K\rangle = a|q\bar{s}\rangle + b|q\bar{s}g\rangle + \dots$$

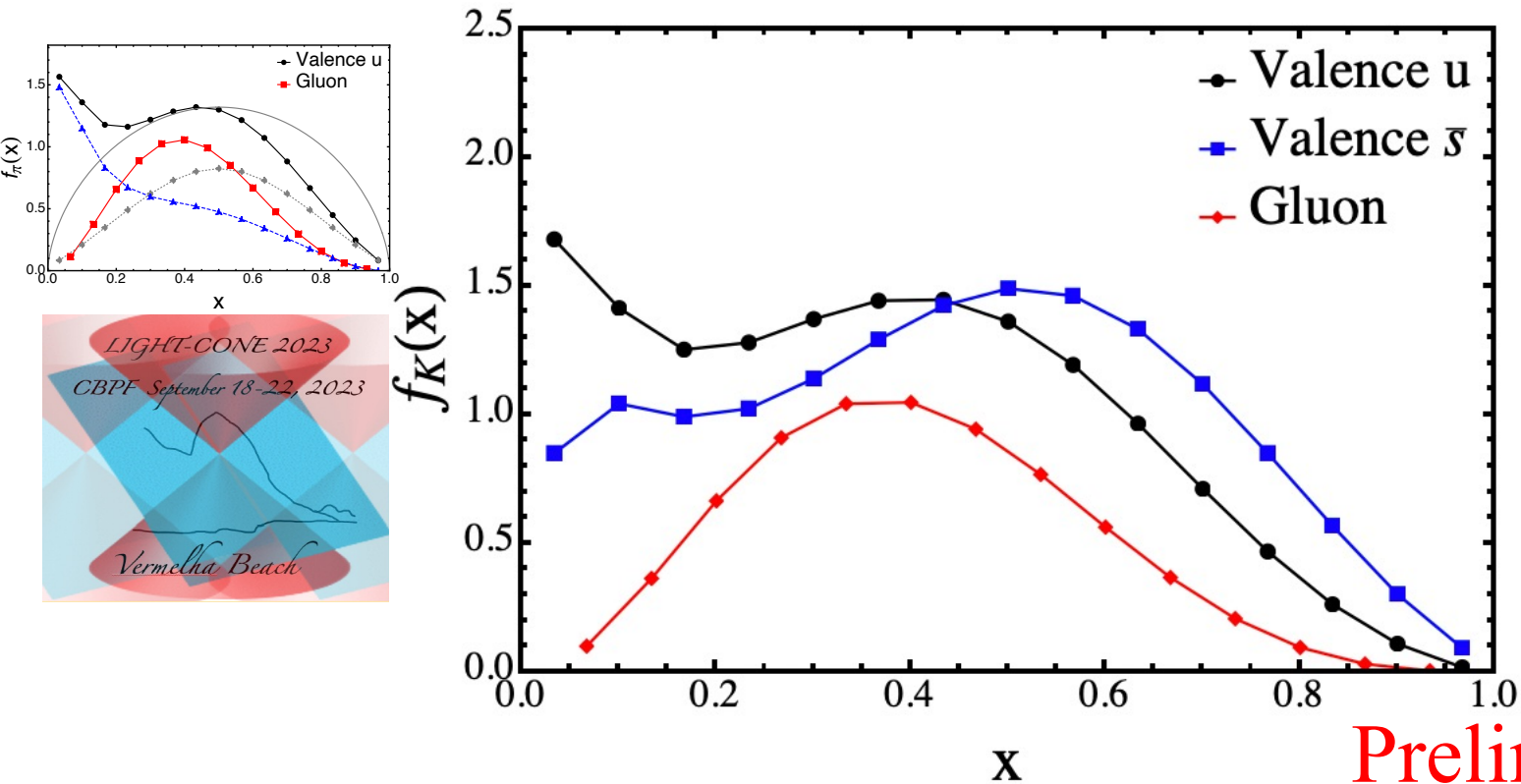


- Endpoint behavior at small x almost agrees with pQCD

Preliminary

Kaon PDF at Model Scale

$$f_i(x) = \sum_{\mathcal{N}, \lambda_i} \int [d\mathcal{X} d\mathcal{P}^\perp]_{\mathcal{N}} \left| \psi_{\{x_i, \vec{p}_{\perp i}, \lambda_i\}}^{\mathcal{N}, M_j=0} \right|^2 \delta(x - x_i) \quad |K\rangle = a|q\bar{s}\rangle + b|q\bar{s}g\rangle + \dots$$



Preliminary

$\pi: \mu_{\text{OBLFQ}}^2 = 0.34 \text{ GeV}^2$	$\langle x \rangle_{\text{gluon}} = 0.216;$	$\langle x \rangle_{\text{val. } u} = 0.392$
$K: \mu_{\text{OBLFQ}}^2 = 0.42 \text{ GeV}^2$	$\langle x \rangle_{\text{gluon}} = 0.193;$	$\langle x \rangle_{\text{val. } u} = 0.363; \quad \langle x \rangle_{\text{val. } \bar{s}} = 0.444$

Kaon PDF with QCD Evolution

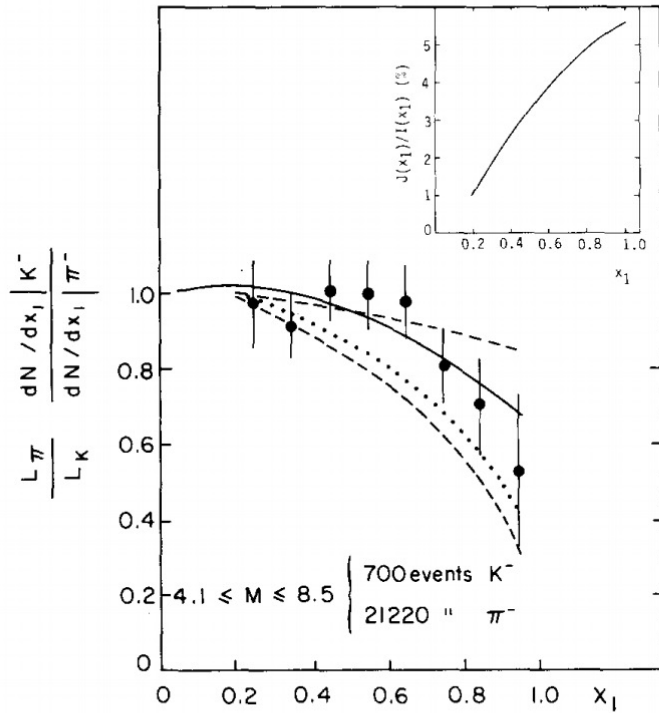
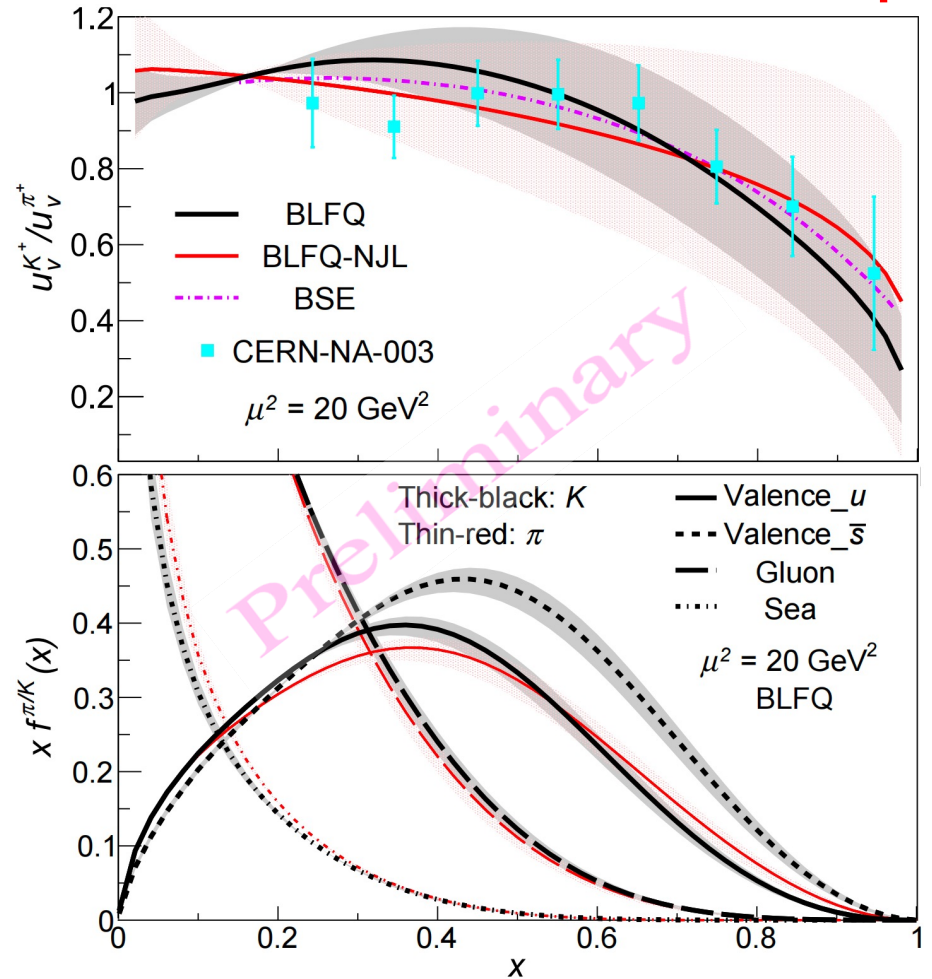


Fig. 2. The data points represent $(L_\pi/L_K)(dN/dx_1)_K/(dN/dx_1)_\pi$ as defined by eq. (4). The dashed curves represent the limits of the ratio $[\bar{u}_K(x_1)/\bar{u}_\pi(x_1)]C(x_1)^{-1}$ where $C(x_1)$ is defined in eq. (3), \bar{u}_K/\bar{u}_π and s_K/\bar{u}_K are taken from ref. [5], and the ratio $J(x_1)/I(x_1)$ is shown in the insert. The upper (lower) curve corresponds to $A = 1/8$ ($A = 1/2$). The dotted and solid curves represent the ratio \bar{u}_K/\bar{u}_π from refs. [6] and [7], respectively.

[Phys. Lett. B 93 (1980) 354]

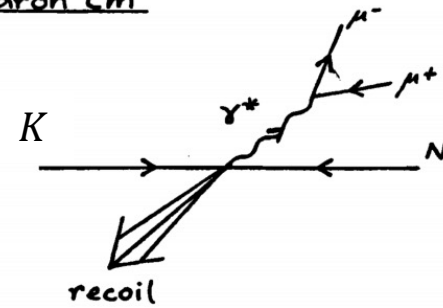
$$|K\rangle = a|q\bar{s}\rangle + b|q\bar{s}g\rangle + \dots$$



Agree with experimental results

Drell-Yan Cross Section

hadron cm

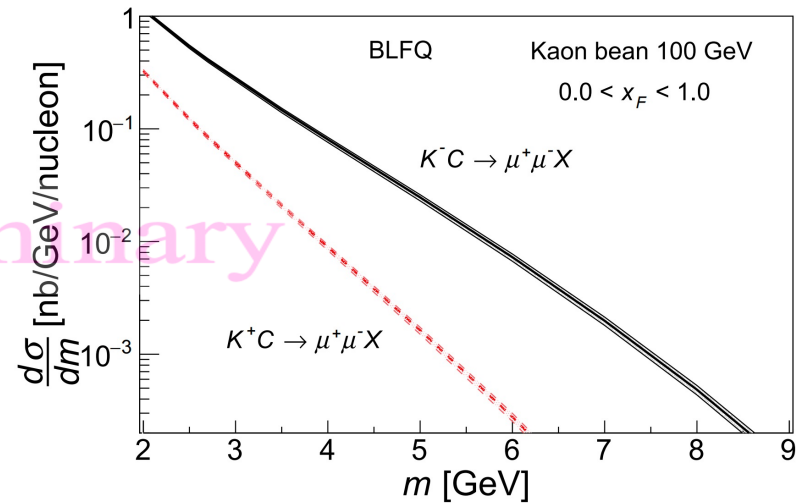
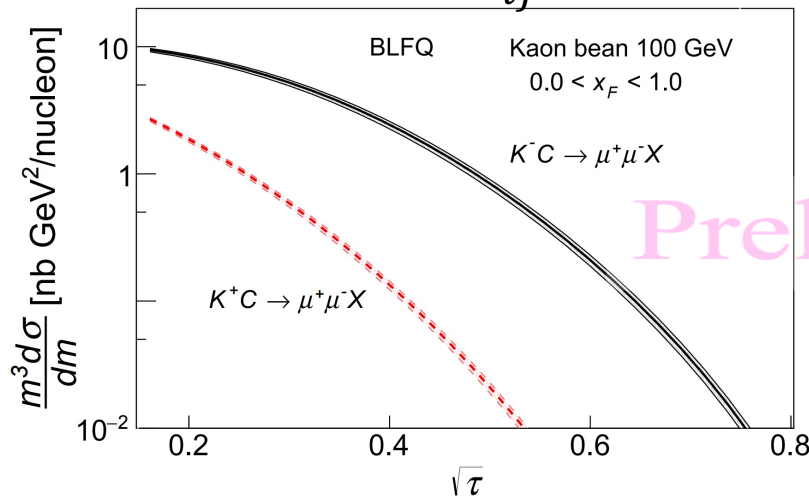


[S. D. Drell and T.-M. Yan, PRL (1970)]

[T. Becher et al, JKEP07(2008)030]; [P. C. Barry et al, PRL121(2018)152001]

[C. Anastasiou et al, PRL91(2003)182002]

$$\frac{m^3 d^2\sigma}{dm dY} = \frac{8\pi\alpha^2 m^2}{9 s} \sum_{ij} dx_1 dx_2 \tilde{C}_{ij}(x_1, x_2, s, m, \mu_f) f_{i/K}(x_1, \mu_f) f_{j/N}(x_2, \mu_f)$$



CERN-AMBER

[CERN-SPSC-2019-022 /SPSC-P-360]

Program	Physics Goals	Beam Energy [GeV]	Beam Intensity [s ⁻¹]	Trigger Rate [kHz]	Beam Type	Target	Earliest start time, duration	Hardware additions
Drell-Yan (RF)	Kaon PDFs & Nucleon TMDs	~100	10 ⁸	25-50	K [±] , p̄	NH ₃ , C/W	2026 2-3 years	"active absorber", vertex detector
Primakoff (RF)	Kaon polarisability & pion life time	~100	5 · 10 ⁶	> 10	K ⁻	Ni	non-exclusive 2026 1 year	
Prompt Photons (RF)	Meson gluon PDFs	≥ 100	5 · 10 ⁶	10-100	K [±] , π [±]	LH2, Ni	non-exclusive 2026 1-2 years	hodoscope
K-induced Spectroscopy (RF)	High-precision strange-meson spectrum	50-100	5 · 10 ⁶	25	K ⁻	LH2	2026 1 year	recoil TOF, forward PID
Vector mesons (RF)	Spin Density Matrix Elements	50-100	5 · 10 ⁶	10-100	K [±] , π [±]	from H to Pb	2026 1 year	

Experiment	Target type	Beam type	Beam intensity (part/sec)	Beam energy (GeV)	DY mass (GeV/c ²)	DY events μ ⁺ μ ⁻	DY events e ⁺ e ⁻
NA3	6 cm Pt	K ⁻		200	4.2 – 8.5	700	0
This exp.	100 cm C	K ⁻	2.1 × 10 ⁷	80	4.0 – 8.5	25,000	13,700
				100	4.0 – 8.5	40,000	17,700
				120	4.0 – 8.5	54,000	20,700
This exp.	100 cm C	π ⁻	4.8 × 10 ⁷	80	4.0 – 8.5	2,800	1,300
				100	4.0 – 8.5	5,200	2,000
				120	4.0 – 8.5	8,000	2,400

[Jiangshan Lan, Jialin Chen et al, in preparation]

Kaon GPD



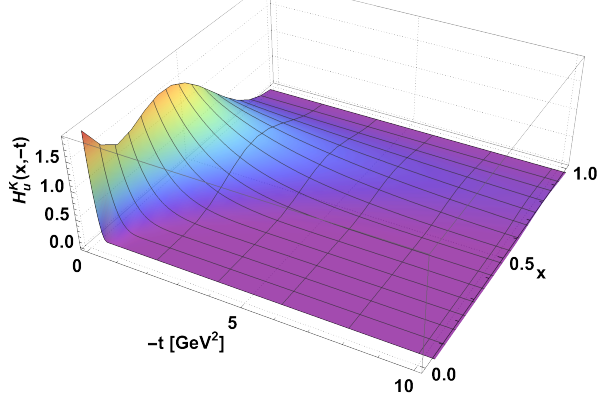
[M. Diehl, Phys. Rep. 388 (2003) 41-277]

$$|K\rangle = a|q\bar{s}\rangle + b|q\bar{s}g\rangle + \dots$$

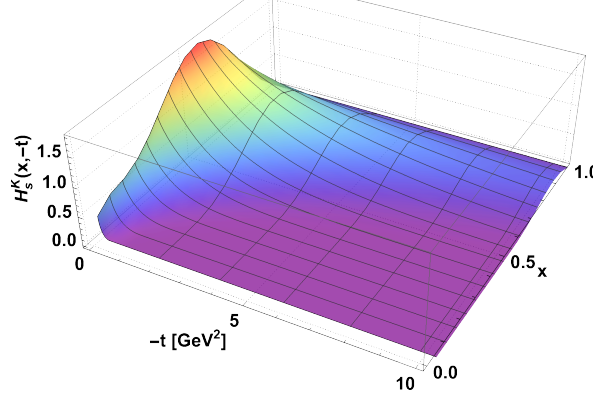
$$H_K^q(x, \xi = 0, t) = \frac{1}{2} \int \frac{dz^-}{2\pi} e^{ixP^+z^-} \left\langle K, P + \frac{\Delta}{2} \left| \bar{q} \left(-\frac{Z}{2} \right) \gamma^+ q \left(\frac{Z}{2} \right) \right| K, P - \frac{\Delta}{2} \right\rangle_{\substack{z^+=0 \\ z_\perp=0}}$$

$$H_K^g(x, \xi = 0, t) = \frac{1}{P^+} \int \frac{dz^-}{2\pi} e^{ixP^+z^-} \left\langle K, P + \frac{\Delta}{2} \left| G^{+\mu} \left(-\frac{Z}{2} \right) G_\mu^+ \left(\frac{Z}{2} \right) \right| K, P - \frac{\Delta}{2} \right\rangle_{\substack{z^+=0 \\ z_\perp=0}}$$

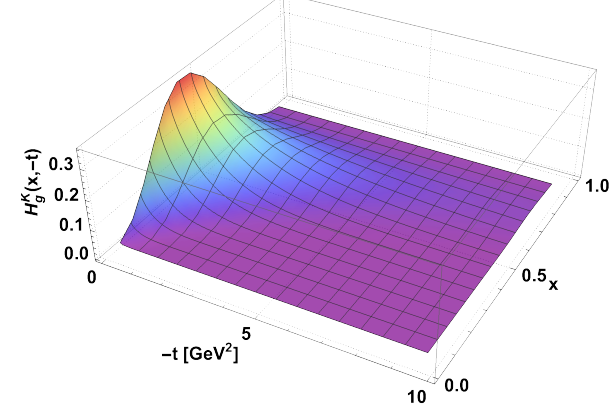
Quark u



Quark \bar{s}



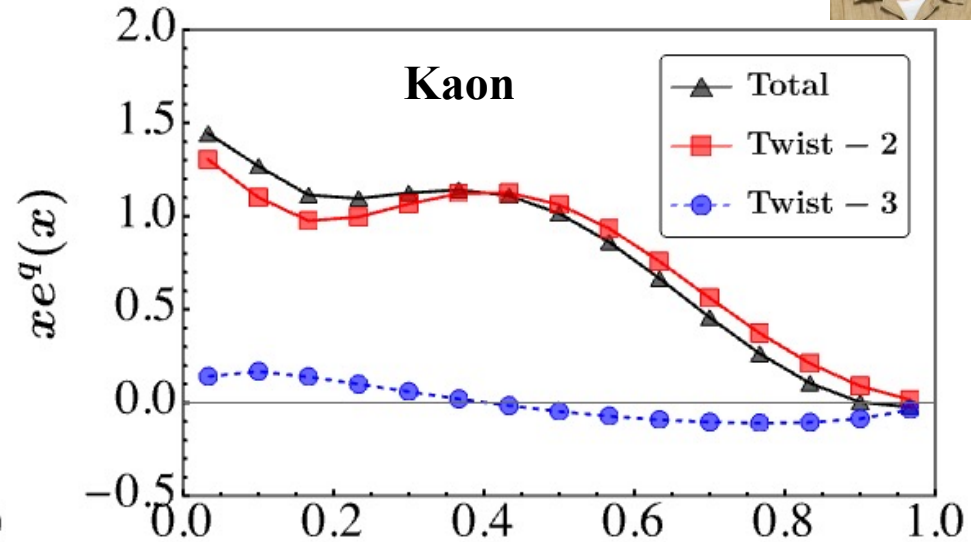
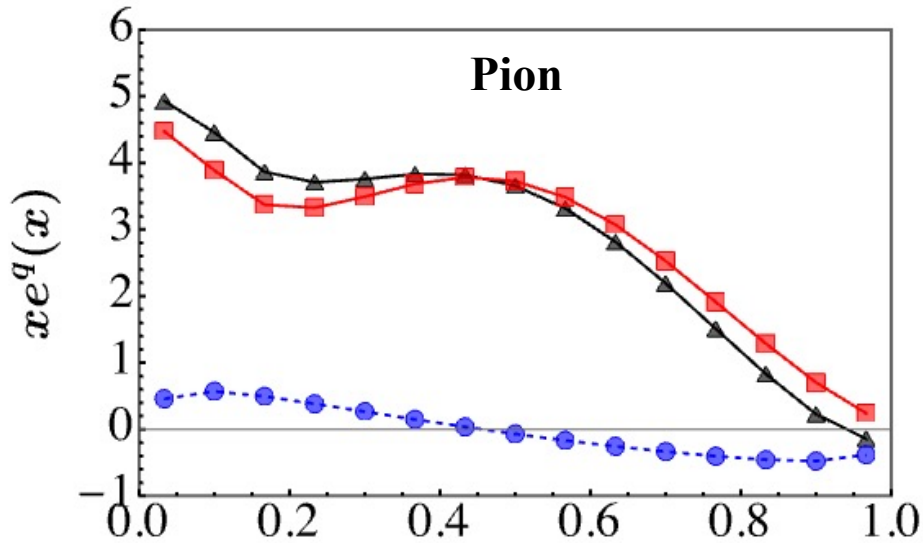
Gluon



- Quark u content enhanced at small x with $|q\bar{s}g\rangle$
- Falls slowly at larger x
- Emerge at larger x range for larger $-t$

Preliminary

Twist-3 xPDFs of Pion & Kaon



[Z. Zhu et al, PLB 839 (2023) 137808]

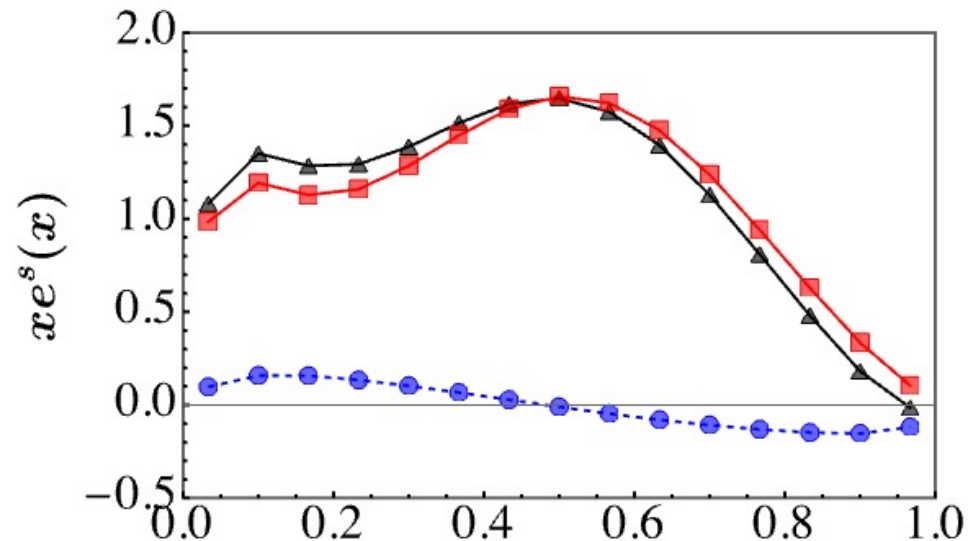
Sum rules

$$\int dx x e^q(x) = \frac{m_q}{M} N_q$$

$$\int dx f_1^q(x) = N_q$$

$$e(x, k_\perp) = \frac{m}{M} \frac{f_1(x, k_\perp)}{x} + \tilde{e}(x, k_\perp),$$

$$\int dx x \tilde{e}(x) = 0$$



➤ BLFQ can provide twist-3 structures which satisfy QCD sum rules

Twist-3 xPDFs of Pion & Kaon

X. Ji

[X.D. Ji, NPB (2020) 115181]

Nuclear Physics B 960 (2020) 115181

where

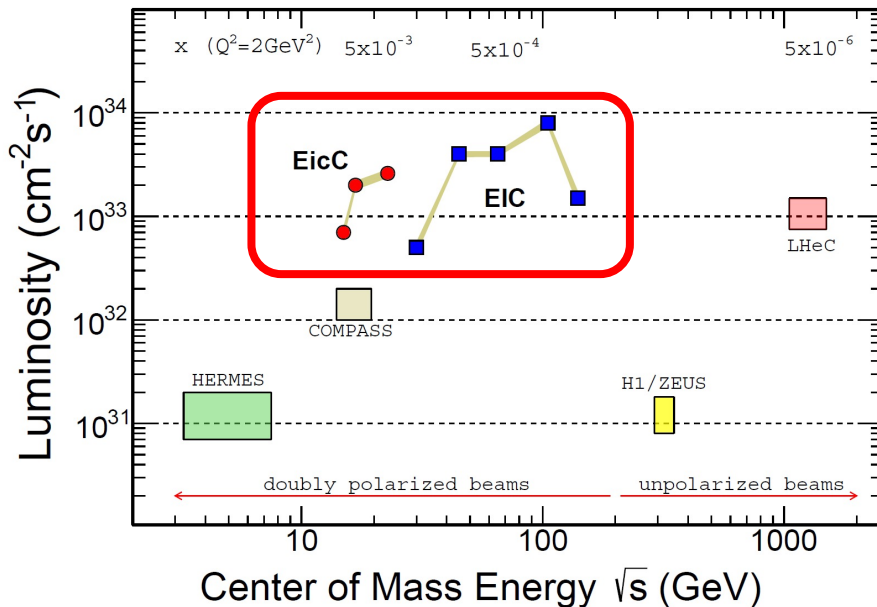
$$M = M_q^{\text{LF}} + M_g^{\text{LF}} + M_a^{\text{LF}} \quad (14)$$

$$M_q^{\text{LF}} = (a + b)M/2 \quad (14)$$

$$M_g^{\text{LF}} = (1 - a)M/2 \quad (15)$$

$$M_a^{\text{LF}} = (1 - b)M/2, \quad (16)$$

respectively, with a is the fraction of the proton momentum carried by quarks $a = \sum_q \int dx x q(x)$, and $b = \sum_q \sigma_q(m_q/M)$. In the massless limit, the quark and gluon kinetic motions contribute the fractions of the proton mass, $a/4$ and $(1 - a)/4$, respectively, and the anomaly gives $1/2$.



[Front.Phys.(Beijing) 16 (2021) 6, 64701]

Low twist

$$a = \sum_q \int dx x f_1^q(x)$$

High twist

$$b = \sum_q \sigma_q(m_q/M) \quad \sigma_q = \int_{-1}^1 dx e_q(x, \mu)$$

➤ High twist structures contribute to hadron structure in the EIC era.

Conclusion & Outlook

- Light-front Hamiltonian approach: **Mass Spectrum** \leftrightarrow **Structure**
- Compared to NJL interaction, dynamical gluon in light meson:
 - ✓ Explains the properties of excited/exotic states such as $\pi(1300)$, $\pi_1(1400)$
 - ✓ Describes EMFF, $F(Q^2) \propto 1/Q^2$ for large Q^2
 - ✓ Improves endpoint behavior in PDF/PDA
 - ✓ Generates more gluon at moderate x /less gluon at small x
 - ✓ Improves agreement on J/ψ production cross section with experimental data
- $\pi - \rho$ mass splitting \sim a large spin-flip matrix element \sim a peak at low- x for quark PDF
- Preliminary results on **gluon** GPDs and TMDs of light mesons
- Light meson \Rightarrow Strangeonia and strange mesons
- Beyond leading twist structure needs to be studied in the EIC era

-
- Systematically expandable by including higher Fock sectors

$$|\text{Meson}\rangle = a|q\bar{q}\rangle + b|q\bar{q}g\rangle + c|q\bar{q}q\bar{q}\rangle + d|q\bar{q}gg\rangle + e|gg\rangle + \dots$$



Welcome to visit us !

High Intensity Heavy-ion Accelerator Facility (HIAF)



1-2 Postdoctoral Positions
✉ xbzhao@impcas.ac.cn

2023

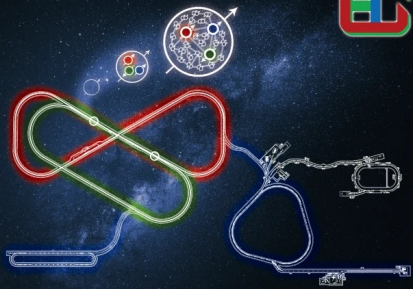


HIAF



New Campus Huizhou, IMP

EicC



Polarized Electron Ion Collider in China
(EicC)